Electronic supplementary information (ESI)

Supramolecular Polymerization of BODIPY Dyes Extended with Rationally designed Pyrazole-based Motif

Youzhi Zhang, Na Zhou, Xiaolin Zhu*, Xiaoming He*

*To whom correspondence should be addressed

Key Laboratory of Applied Surface and Colloid Chemistry (Ministry of Education), School of Chemistry and Chemical Engineering, Shaanxi Normal University, Xi'an 710119, P.R. China

*Corresponding Author Email: xmhe@snnu.edu.cn, xiaolinchem@snnu.edu.cn

Experimental section

Synthesis
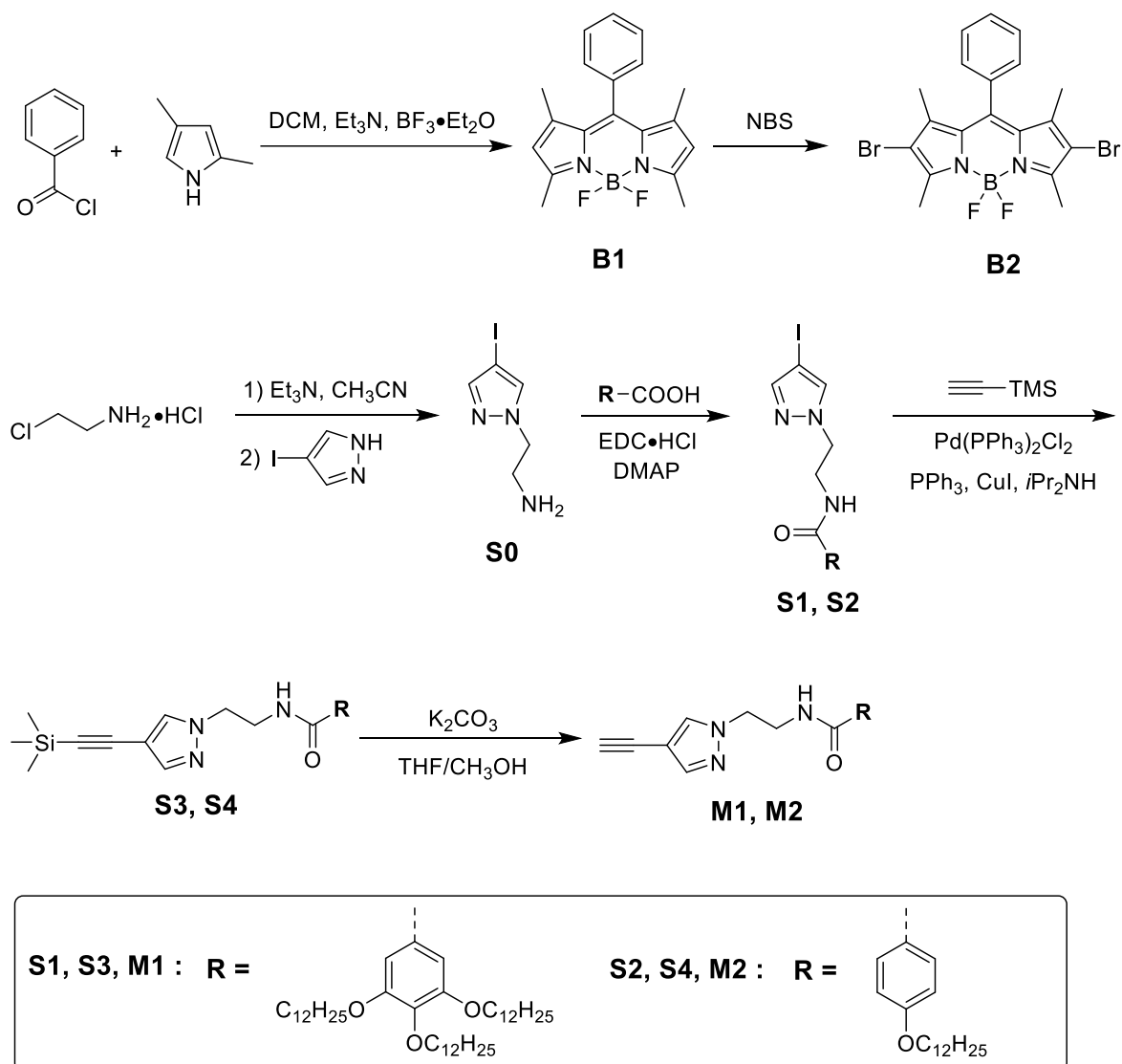
Scheme S1. Synthesis of precursors.

BODIPY precursors (**B1** and **B2**)[S1] and R-COOH starting materials,[S2] such as 3,4,5-tris(dodecyloxy)benzoic acid and 4-(dodecyloxy) benzoic acid were synthesized according to the literatures.

Synthesis of S0. To a suspension of 2-chloroethylamine hydrochloride (6.0 g, 51.7 mmol) in 80 mL acetonitrile, triethylamine (7.4 mL, 52.4 mmol) was added. The mixture was stirred at R.T. for 2 h. A white precipitate was formed during the reaction and was removed from reaction mixture by

filtration and washed with 40 mL acetonitrile. The collected acetonitrile solution of 2-chloroethyl amine was concentrated to half volume under vacuum.

To another 250 mL round bottle flask was charged with 4-iodopyrazole (5.0 g, 25.8 mmol), NaOH (3.1 g, 77.5 mmol) and acetonitrile (40 mL). The mixture was stirred for 30 min at R.T. and then heated up to 75 °C. Then the acetonitrile solution of 2-chloroethyl amine was added dropwise into the solution over 30 min, and the mixture was stirred at 75 °C for 24 h. After cooled to R.T., the formed precipitate was removed by filtration. The filtrate was concentrated in vacuo to obtain pale-yellow oil 6.0 g (Yield: 98 %). ^{1}H NMR (400 MHz, CDCl$_3$): δ (ppm) = 7.52 (s, 1H; CH), 7.48 (s, 1H; CH), 4.16 (t, J = 3.6 Hz; 2H; CH_2), 3.11 (t, J = 3.6 Hz, 2H; CH_2). ^{13}C NMR (100 MHz, CDCl$_3$): δ (ppm) = 144.62, 134.19, 55.94, 55.41, 41.97. HRMS (ESI) calcd for [C$_5$H$_9$IN$_3$]$^+$, 237.9836; found, 237.9839.

Synthesis of S1. S0 (4.74 g, 20 mmol), 3,4,5-tris(dodecyloxy)benzoic acid (14.04 g, 20.8 mmol), EDC·HCl (4.38 g, 22.8 mmol) and 4-DMAP (1.78 g, 14.6 mmol) were dissolved in CH$_2$Cl$_2$ (120 mL), and the reaction mixture was stirred at R.T. for 24 h. Then the reaction mixture was diluted with CH$_2$Cl$_2$ and the organic layer was washed with brine three times. The collected organic layer was dried over anhydrous MgSO$_4$ and concentrated in *vacuo*. Purification of the crude product by column chromatography (silica gel, CH$_2$Cl$_2$/ MeOH = 20:1 (v/v) to afford the desired product as a white solid (Yield: 12.5 g, 70 %). ^{1}H NMR (400 MHz, CDCl$_3$): δ (ppm) = 7.55 (s, 1H; CH), 7.46 (s, 1H; CH), 6.90 (s, 2H; ArH), 6.67 (t, J = 5.6 Hz, 1H; NH), 4.36 (t, J = 5.6 Hz, 2H; CH_2), 3.99 (m, 6H; OCH_2), 3.83 (m, 2H; CH_2), 1.84-1.69 (m, 6H; CH_2), 1.47 (m, 6H; CH_2), 1.26 (s, 48H; CH_2), 0.88 (t, J = 7.2 Hz, 9H; CH_3). ^{13}C NMR (100 MHz, CDCl$_3$): δ (ppm) = 167.72, 153.25, 145.27, 141.44, 134.76, 129.07, 105.68, 73.65, 69.44, 56.28, 51.53, 40.41, 32.08, 30.46, 29.80, 29.52, 26.25, 22.84, 14.26. HRMS (ESI) calcd for [C$_{48}$H$_{85}$IN$_3$O$_4$]$^+$, 894.5579; found, 894.5592.

Synthesis of S2. The procedure was similar to that used to prepare **S1**, except 4-dodecyloxy benzoic acid (6.38 g, 20.8 mmol) was used in place of 3,4,5-tris(dodecyloxy)benzoic acid. Yield: 6.8 g (65 %). ^{1}H NMR (400 MHz, CDCl$_3$): δ (ppm) = 7.68 (d, 2H, J = 8.8 Hz; ArH), 7.54 (s, 1H; CH), 7.43 (s, 1H; CH), 6.89 (d, J = 8.8 Hz, 2H; ArH), 6.84 (s, 1H; NH), 4.33 (t, J = 5.6 Hz, 2H; CH_2), 3.97 (t, J = 6.4 Hz, 2H; OCH_2), 3.82 (m, 2H; CH_2), 1.78 (m, 2H; CH_2), 1.44 (m, 2H; CH_2), 1.25 (s, 16H; CH_2), 0.87 (t, J = 7.2 Hz, 3H; CH_3). ^{13}C NMR (100 MHz, CDCl$_3$): δ (ppm) = 167.33, 162.04, 145.16, 134.62, 128.84, 126.01, 114.36, 68.29, 56.25, 51.59, 40.23, 32.01, 29.75, 29.73, 29.69, 29.66, 29.47, 29.45, 29.22, 26.09, 22.79, 14.24. HRMS (ESI) calcd for [C$_{24}$H$_{37}$IN$_3$O$_2$]$^+$, 526.1925; found, 526.1932.

Synthesis of S3. To a two-neck round-bottom flask equipped with a condenser was charged with **S1** (2.0 g, 2.24 mmol), PdCl$_2$(PPh$_3$)$_2$ (80 mg, 0.12 mmol), CuI (44 mg, 0.24 mmol), PPh$_3$ (60 mg, 0.24 mmol). This mixture was put under three vacuum-N$_2$ cycles before adding degassed *i*Pr$_2$NH (40 mL).

After stirring for 10 min, (trimethylsilyl)acetylene (0.94 mL, 6.72 mmol) was injected into the flask and the mixture was heated at 70 °C for 24 h. The formed solid was removed by filtration and washed with THF. The solvent was removed under reduced pressure and the crude product was purified on a silica-gel column [silica gel, CH_2Cl_2/ MeOH = 20:1 (v/v)] to give compound S3 (1.3 g, 68 %) as a white solid. ^{1}H NMR (400 MHz, CDCl$_3$): δ (ppm) = 7.63 (s, 1H; CH), 7.54 (s, 1H; CH), 6.90 (s, 2H; ArH), 6.71 (m, 1H; NH), 4.31 (m, 2H; CH_2), 3.98 (m, 2H; OCH_2), 3.85 (m, 2H; CH_2), 1.80 (m, 6H; CH_2), 1.46 (m, 6H; CH_2), 1.26 (s, 48H; CH_2), 0.87 (t, J = 6.8 Hz, 9H; CH_3), 0.21 (s, 9H; CH_3). ^{13}C NMR (100 MHz, CDCl$_3$): δ (ppm) = 167.71, 153.21, 143.14, 141.37, 133.51, 129.01, 105.65, 95.81, 95.69, 73.63, 69.37, 51.36, 40.24, 32.07, 30.45, 29.79, 29.51, 26.24, 22.94, 14.26, 0.10. HRMS (ESI) calcd for [C$_{53}$H$_{94}$N$_3$O$_4$Si]$^+$, 864.7008; found, 864.7017.

Synthesis of S4. The procedure was similar to that used to prepare **S3**, except **S2** (1.2 g, 2.24 mmol) was used in place of **S1**. Yield: 0.72 g (64 %). ^{1}H NMR (400 MHz, CDCl$_3$): δ (ppm) = 7.68 (s, 1H; CH), 7.66 (d, J = 7.2 Hz, 2H; ArH), 7.53 (s, 1H; CH), 6.90 (d, J = 8.4 Hz, 2H; ArH), 6.72 (t, J = 5.2 Hz,1H; NH), 4.31 (t, J = 5.6 Hz, 2H; CH_2), 3.97 (t, J = 6.4 Hz, 2H; OCH_2), 3.84 (m, 2H; CH_2), 1.78 (m, 2H; CH_2), 1.44 (m, 2H; CH$_2$), 1.26 (s, 16H; CH$_2$), 0.87 (t, J = 6.8 Hz, 3H; CH$_3$), 0.21 (s, 9H, CH$_3$). ^{13}C NMR (100 MHz, CDCl$_3$): δ (ppm) = 167.32, 162.10, 143.18, 133.44, 128.87, 126.02, 114.40, 103.60, 95.94, 95.59, 68.32, 51.52, 40.16, 32.04, 29.78, 29.48, 29.25, 26.12, 22.82, 14.26, 0.10. HRMS (ESI) calcd for [C$_{29}$H$_{46}$N$_3$O$_2$Si]$^+$, 496.3354; found, 496.3356.

Synthesis of M1. **S3** (0.86 g, 1.0 mmol) and K$_2$CO$_3$ (0.68 g, 5.0 mmol) were added to THF (10 mL) and methanol (10 mL), and the mixture was stirred for 6 h at R.T. After the reaction completed (monitored by TLC), the mixture was extracted with CH$_2$Cl$_2$ and washed with water three times. The combined organic layer was dried over anhydrous Na$_2$SO$_4$ and concentrated under reduced pressure. The solid was dissolved in minimum volume of CH$_2$Cl$_2$ and re-precipitated in methanol. The mixture was kept at ice-water bath for 1 h and the white precipitate was collected by filtration (Yield: 0.72 g, 92 %). ^{1}H NMR (400 MHz, CDCl$_3$): δ (ppm) = 7.61 (s, 1H, CH), 7.56 (s, 1H; CH), 6.90 (s, 2H; ArH), 6.89 (s, 1H; NH), 4.29 (t, J = 5.4 Hz, 2H, CH$_2$), 3.95 (m, 2H, OCH$_2$), 3.80 (m, 2H, CH$_2$), 2.98 (s, 1H, C≡CH), 1.80-1.69 (m, 6H, CH$_2$), 1.46-1.42 (m, 6H, CH$_2$), 1.25 (s, 48H, CH$_2$), 0.86 (t, J = 7.2 Hz, 9H, CH$_3$). ^{13}C NMR (100 MHz, CDCl$_3$): δ (ppm) = 167.76, 153.22, 143.19, 141.36, 133.74, 129.03, 105.62, 102.43, 74.82, 73.63, 69.36, 51.36, 40.21, 32.07, 30.45, 29.79, 29.51, 26.23, 22.93, 14.26. HRMS (ESI) calcd for [C$_{50}$H$_{86}$N$_3$O$_4$]$^+$, 792.6613; found, 792.6617.

Synthesis of M2. The procedure was similar to that used to prepare **M1**, except **S4** (0.5 g, 1.0 mmol) was used in place of **S3**. Yield: 0.4 g (90 %). ^{1}H NMR (400 MHz, CDCl$_3$): δ (ppm) = 7.69 (s, 1H; CH), 7.67 (d, J = 2.0 Hz, 2H; ArH), 7.55 (s, 1H; CH), 6.90 (d, J = 8.8 Hz, 2H; ArH), 6.75 (t, J =

5.2 Hz, 1H; NH), 4.32 (t, J = 5.6 Hz, 2H; CH_2), 3.98 (t, J = 6.4 Hz, 2H; OCH_2), 3.86 (m, 2H; CH_2), 3.00 (s, 1H; C≡CH), 1.78 (m, 2H; CH_2), 1.44 (m, 2H; CH_2), 1.26 (s, 16H; CH_2), 0.87 (t, J = 7.2 Hz, 3H; CH_3). ^{13}C NMR (100 MHz, CDCl$_3$): δ (ppm) =167.21, 161.98, 143.09, 133.52, 128.72, 125.89114.29, 102.23, 78.47, 74.82, 68.20, 51.41, 40.03, 31.92, 29.65, 29.35, 29.12, 25.99, 22.69, 14.13. HRMS (ESI) calcd for [C$_{26}$H$_{38}$N$_3$O$_2$]$^+$, 424.2959; found, 424.2964.

Synthesis of 1. To a two-neck round-bottom flask equipped with a condenser was charged with **M1** (250 mg, 0.32 mmol), **B2** (72.3 mg, 0.15 mmol), PdCl$_2$(PPh$_3$)$_2$ (11 mg, 0.015 mmol), CuI (6 mg, 0.03 mmol), PPh$_3$ (8 mg, 0.03 mmol) and a solvent of THF/iPr$_2$NH (1:1, v/v, 20 mL). The flask was degassed by three times of freeze-pump-thaw cycles and refilled with N$_2$ before stirring at 70 °C for 48 h. The solvent was removed under reduced pressure, and the crude product was purified on a silica-gel column [silica gel, CH$_2$Cl$_2$/MeOH = 50:1 (v/v)] to give compound **1** (108 mg, 38 %). ^{1}H NMR (400 MHz, CDCl$_3$): δ (ppm) = 7.63 (s, 2H; CH), 7.55 (s, 2H; CH), 7.52 (m, 3H; ArH), 6.91 (s, 4H; ArH), 6.70 (s, 2H; NH), 4.34 (m, 4H; CH_2), 3.99 (m, 12H; OCH_2), 3.86 (m, 4H; CH_2), 2.67 (s, 2H; CH_3), 1.79 (m, 12H; CH_2), 1.46 (m, 18H; CH_2+CH_3), 1.26 (s, 96H; CH_2), 1.26 (s, 32H; CH_2), 0.87 (t, J = 6.8 Hz, 18H; CH_3). ^{13}C NMR (100 MHz, CDCl$_3$): δ (ppm) = 167.70, 158.37, 153.22, 145.27, 143.88, 142.61, 141.42, 134.56, 132.73, 131.27, 129.48, 129.05, 127.92, 116.30, 105.70, 103.76, 86.84, 82.45, 73.64, 69.41, 51.40, 40.27, 32.08, 30.46, 29.88, 29.85, 29.80, 29.73, 29.52, 26.24, 22.84, 14.26, 13.81, 13.47. HRMS (ESI) calcd for [C$_{119}$H$_{186}$BF$_2$N$_8$O$_8$]$^+$, 1904.4454; found, 1904.4463.

Synthesis of 2. The procedure was similar to that used to prepare **1**, except **M2** (136 mg, 0.32 mmol) was used in place of **M1**. Yield: 70 mg (40 %). ^{1}H NMR (400 MHz, CDCl$_3$): δ (ppm) = 7.69-7.65 (m, 6H; CH+ArH), 7.54 (s, 2H; CH), 7.52 (m, 3H; ArH), 6.91 (d, J = 8.4 Hz, 2H; ArH), 6.69 (s, 2H; NH), 4.33 (m, 4H; CH_2), 3.98 (t, J = 6.4 Hz, 4H; OCH_2), 3.87 (m, 4H; CH_2), 2.67 (s, 6H; CH_3), 1.78 (m, 4H; CH_2), 1.46 (m, 10H; CH_2+CH_3), 1.26 (s, 32H; CH_2), 0.88 (t, J = 6.8 Hz, 6H; CH_3). ^{13}C NMR (100 MHz, CDCl$_3$): δ (ppm) = 167.32, 162.11, 158.36, 143.90, 142.65, 134.55, 132.67, 131.24, 129.46, 128.86, 127.92, 126.03, 116.33, 114.40, 103.64, 86.96, 82.33, 68.34, 51.55, 40.20, 32.05, 29.79, 29.77, 29.73, 29.69, 29.51, 29.48, 29.26, 26.12, 22.83, 14.27, 13.83, 13.48. HRMS (ESI) calcd for [C$_{71}$H$_{90}$BF$_2$N$_8$O$_4$]$^+$, 1167.7152; found, 1167.7131.

Temperature-dependent Isodesmic Model and Cooperative Model in Curve Fitting

(1) Determination of the fraction of aggregates from UV-vis absorption spectra

The fraction of aggregates α(T) at different temperatures can be calculated according to Eq. (1).

$$\alpha(T) = \frac{A(T)-A_M}{A_A-A_M} \quad (1)$$

where $A(T)$ is the measured absorbance at temperature T; A_M and A_A are the absorbances of the monomer and fully aggregated state, respectively.

(2) The isodesmic model

The isodesmic model assumes a single equilibrium constant K_e during all aggregation steps. It is also known as the equal-K model.[S3] For an isodesmic aggregation pathway, the experimental α_{agg} values can be related to temperature by a sigmoidal relation. The sigmoidal function for α ($0 \leq \alpha \leq 1$) can generally be expressed as Eq. (2):

$$\alpha(T) \cong \frac{1}{1+\exp[-0.908\Delta H \frac{T-T_m}{RT_m^2}]} \quad (2)$$

Where T_m is the melting temperature when $\alpha = 0.5$, ΔH is the molar enthalpy release related to the formation of non-covalent intermolecular interactions, and R is the universal gas constant.

Equation (2) could be utilized to fit the experimental data obtained from the UV-vis absorption change at different temperature to obtain ΔH and T_m.

Furthermore, the average stack length DP_N as well as the equilibrium constant K_e can be obtained, with concentration c, by the equation (3) below:

$$DP_N = \frac{1}{\sqrt{1-\alpha(T)}} = \frac{1}{2} + \frac{1}{2}\sqrt{4K_e(T)c_T + 1} \quad (3)$$

(3) The Cooperative model

The cooperative model consists of two steps, nucleation and elongation processes, which are divided by the corresponding elongation temperature T_e. According to the nucleation and elongation model developed and by Meijer and coworkers,[S3,S4] the nucleation ($T < T_e$) and elongation ($T > T_e$) regime are governed by Eq. (4) and (5) respectively.

$$\alpha(T) = \sqrt[3]{K_a}\exp\left\{\left(\frac{2}{3\sqrt[3]{K_a}} - 1\right)\frac{-\Delta H_e}{RT_e^2}(T - T_e)\right\} \quad (4)$$

$$\alpha(T) = \alpha_{SAT}\left\{1 - \exp\left(\frac{-\Delta H_e}{RT_e^2}(T - T_e)\right)\right\} \quad (5)$$

Where ΔH_e is the molecular enthalpy released due to non-covalent interactions during elongation process, T and T_e stand for the absolute temperature and elongation temperature, respectively, K_a is the dimensionless equilibrium constant of the nucleation process at T_e, R is the universal gas constant, α_{SAT} is a parameter that is introduced to prevent the relation $\alpha(T)/\alpha_{SAT}$ surpassing the value of 1.

Determination of the cooperativity factor σ is given by Eq. (6)

$$\sigma = \frac{K_n}{K_e} \quad (6)$$

Where K_n and K_e are the binding constants for the nucleation and elongation steps, respectively.

Mathematical curve fitting for luminescent temperature sensing

Firstly, the thermometric parameters Δ was calculated based on the ratio of the maximum values of peaks. In detail, Δ was determined by the intensity ratios of I_{652}/I_{606} for **1** in response to the variation of temperature in heptane.

Then Δ is fitted employing modified Arrhenius-type equation (7):

$$\Delta = \frac{\Delta_0}{1 + \alpha\exp\left(-\frac{\Delta E}{k_B T}\right)} \quad (7)$$

Where Δ_o is thermometric parameter corresponding to starting temperature. α is the pre-exponential factor. ΔE is the energy gap between the lowest excited state and a crossing point to a non-radiatively decaying state and k_B is the Boltzmann constant. T is the real-time temperature. All calculations were performed using the TeSen software tool.[S5-S7]

The relative thermal sensitivity (S_r) was evaluated using the expression as equation (8). The S_r indicates the relative change of the thermometric parameter per degree of temperature change (% K^{-1}).

$$S_r = 100\% \times \left| \frac{1}{\Delta}\frac{\partial \Delta}{\partial T} \right| \quad (8)$$

The repeatability R was calculated as equation (9):[S5-S7]

$$R = 1 - \frac{\max\left(|\varDelta_{\text{mean}} - \varDelta_i|\right)}{\varDelta_{\text{mean}}} \qquad (9)$$

Where $\varDelta_{\text{mean}}$ is the mean value of the thermometric parameter as obtained from the calibration curve, and $\varDelta_i$ is the value of the thermometric parameter obtained for each considered measurement.

Procedures for self-assembly experiments

Compound **1, 2** were suspended in hydrocarbon-based solvents such as n-hexanes, heptane, and MCH at a concentration of 1×10^{-5} M, gently heated to ensure complete dissolution, then allowed to cool to ambient temperature over 24 h. A drop of each solution was dropcast onto carbon-coated copper grids for analysis by TEM. Atomic force microscopy (AFM) images were collected by dropcasting from solution (1×10^{-5} M) onto carbon coated mica.

Supporting Figures
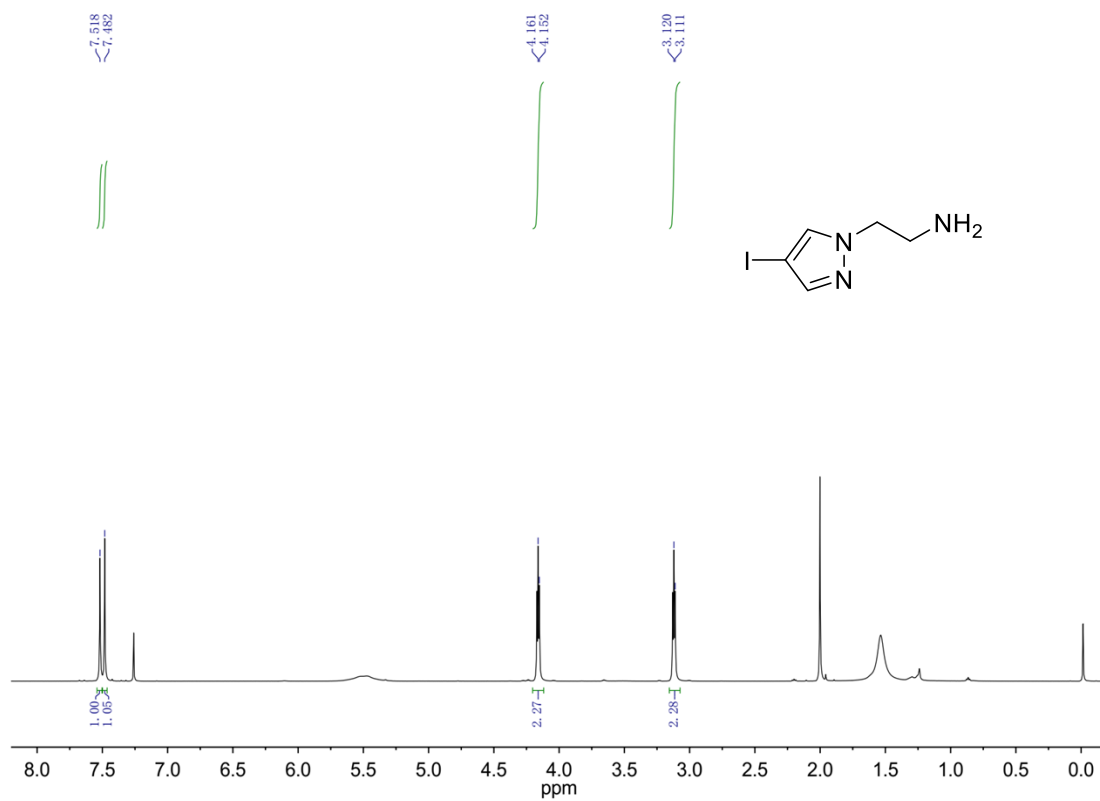
Figure S1. ^{1}H NMR spectrum of **S0** in CDCl$_3$.
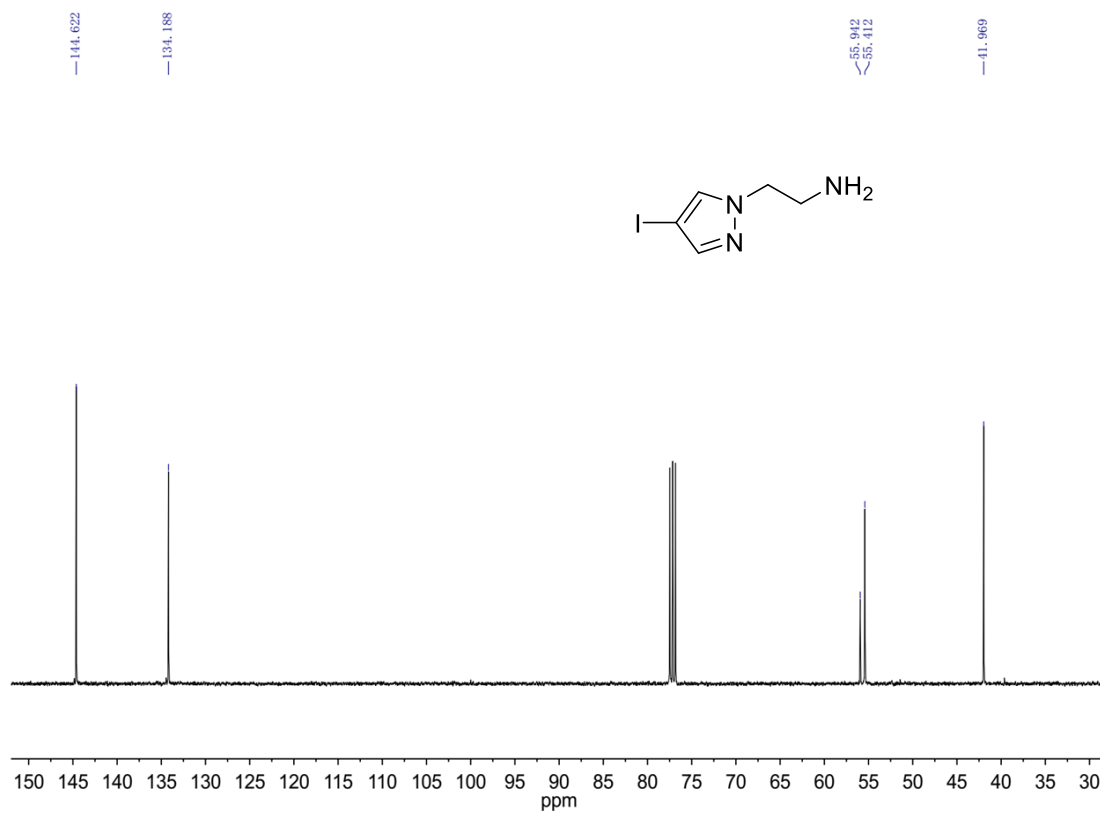
Figure S2. ^{13}C NMR spectrum of **S0** in CDCl$_3$.
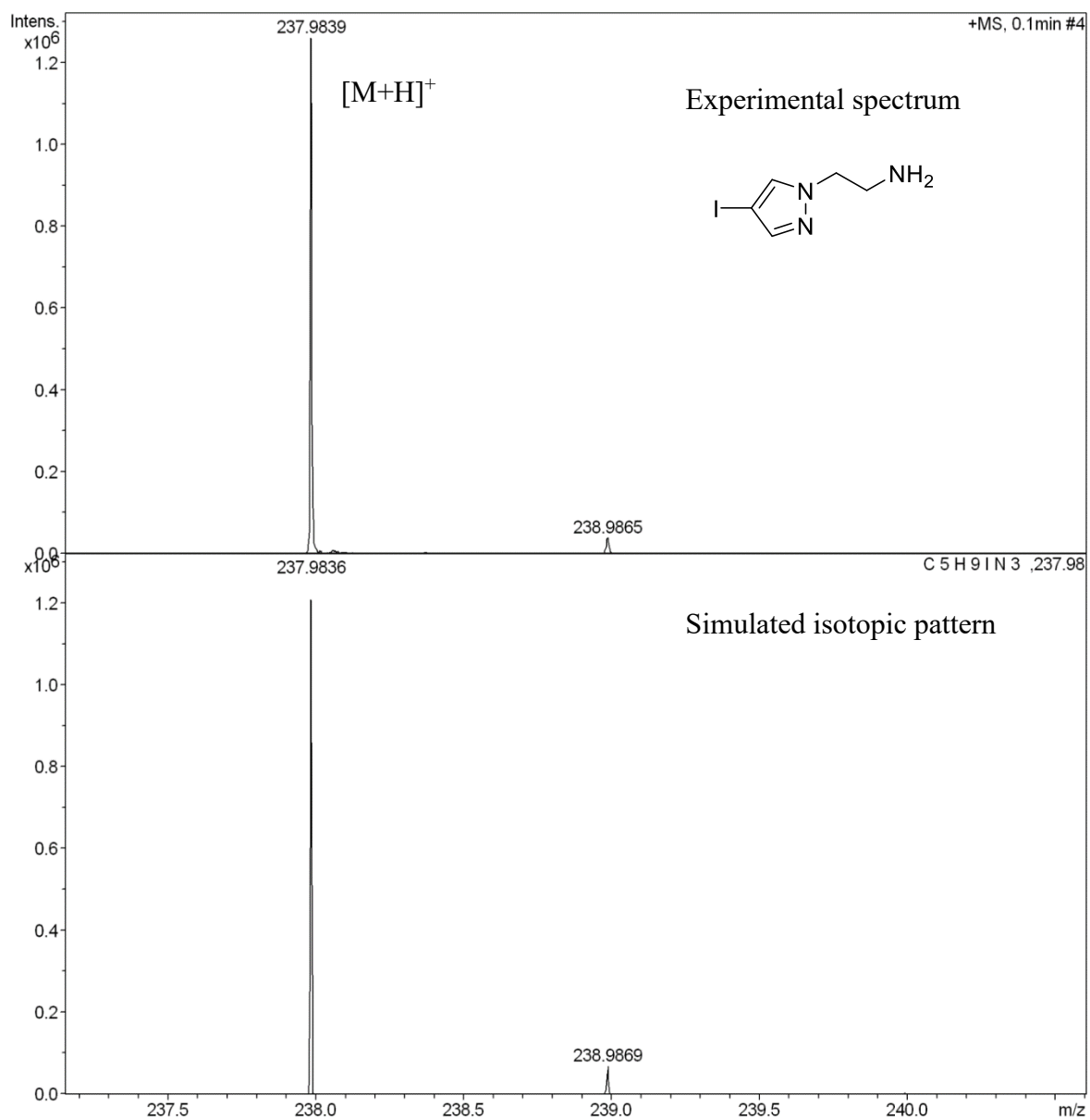
Figure S3. HRMS spectrum of **S0**.
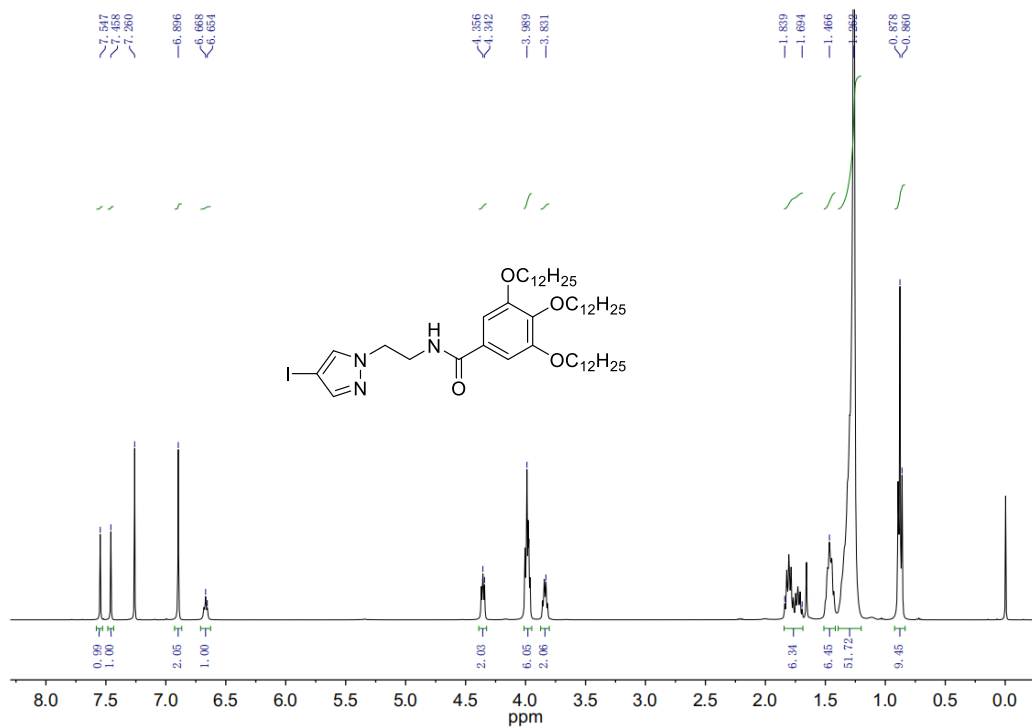
Figure S4. ^{1}H NMR spectrum of **S1** in CDCl$_3$.
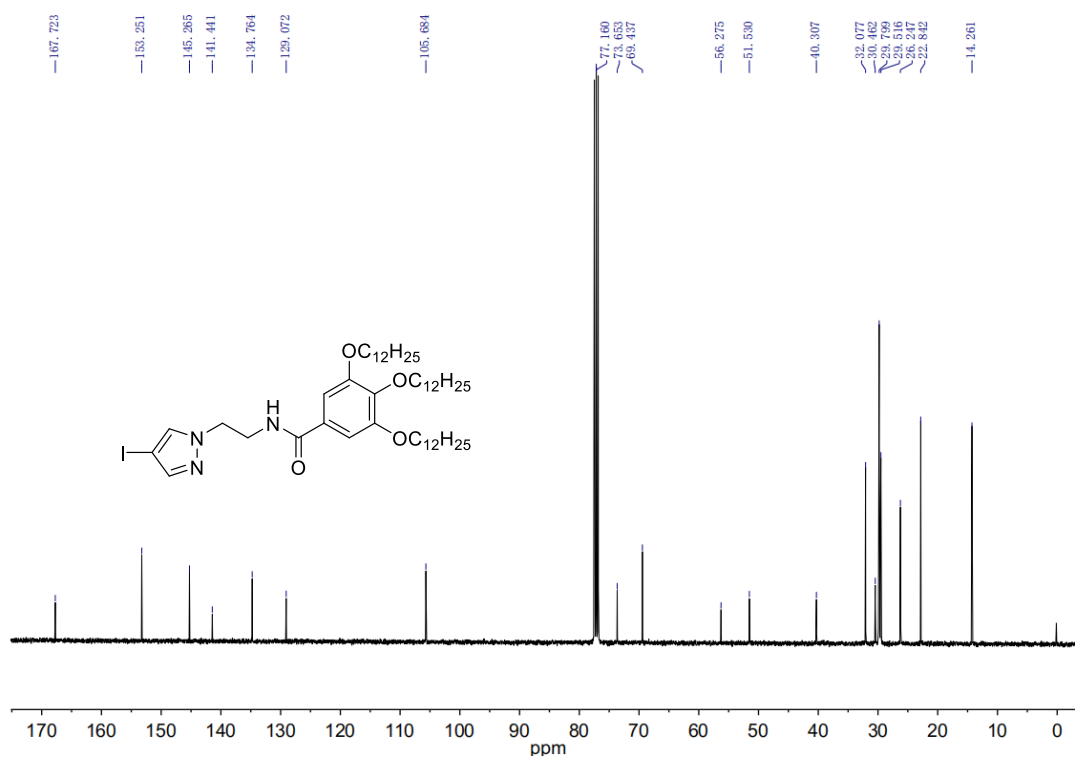
Figure S5. ^{13}C NMR spectrum of **S1** in CDCl$_3$.
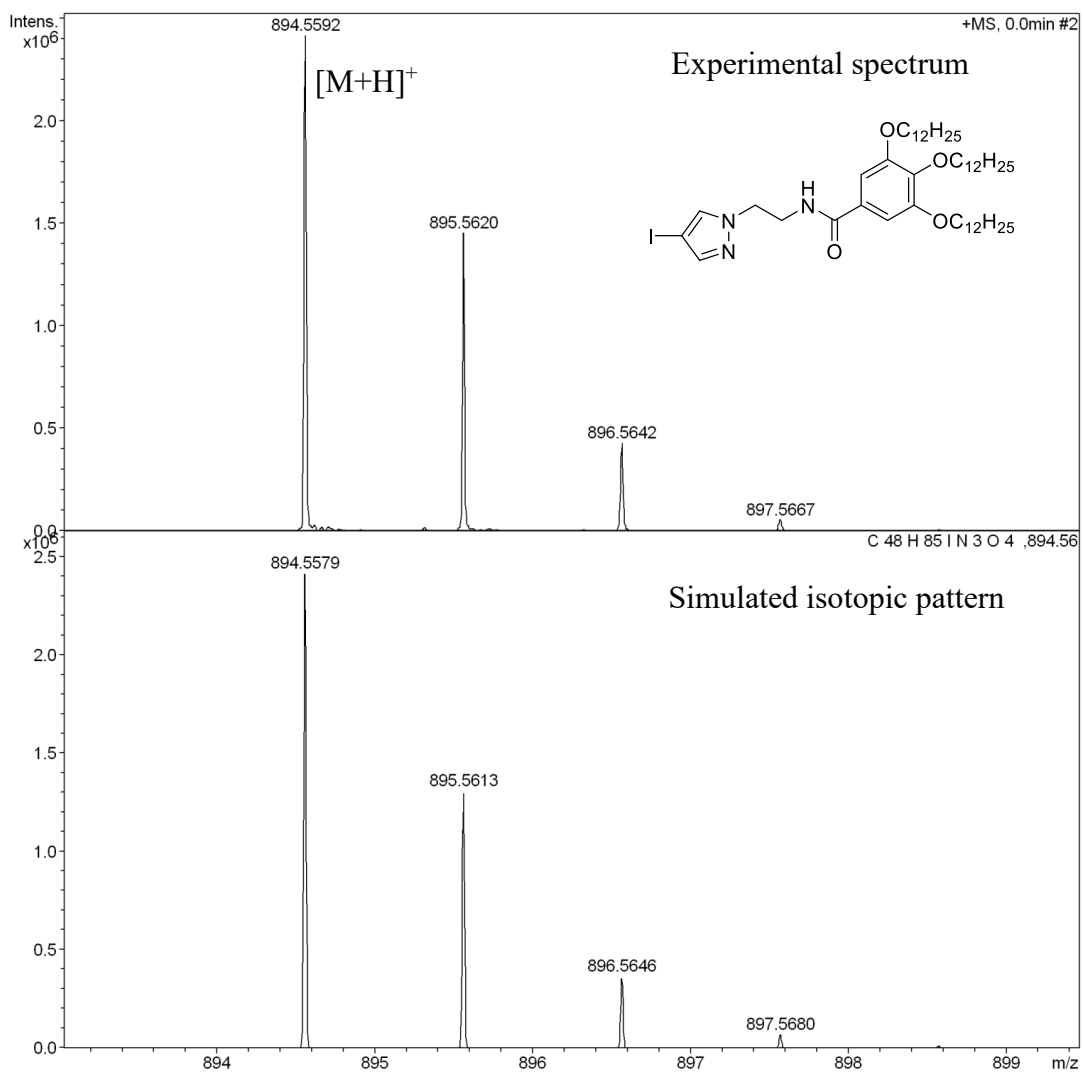
Figure S6. HRMS spectrum of **S1**.
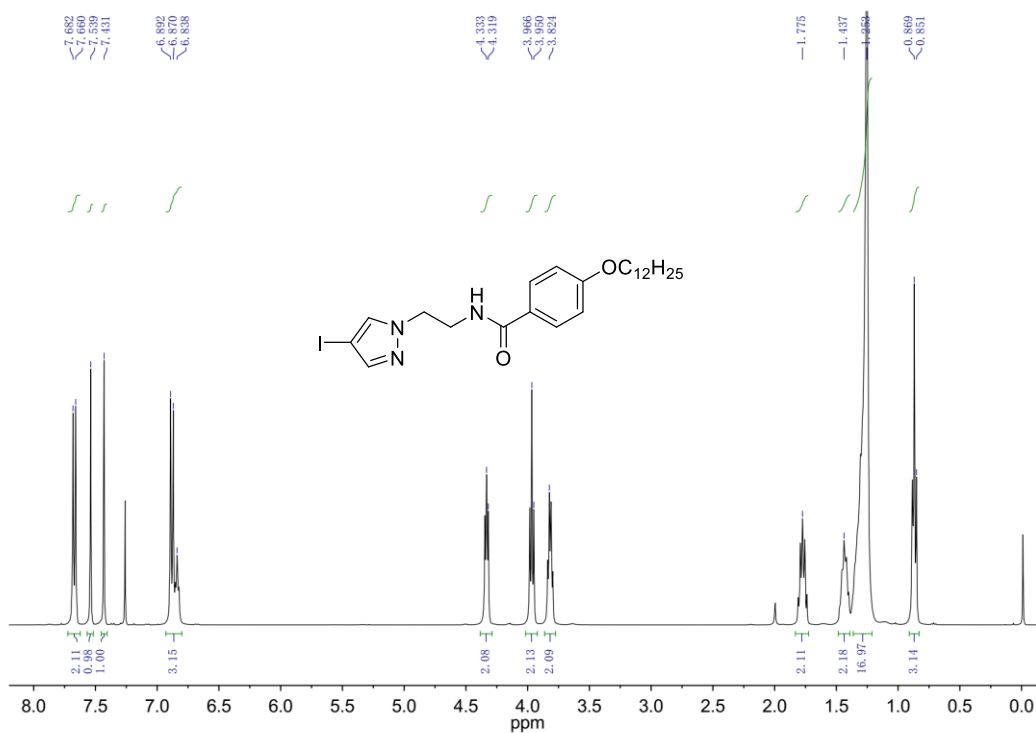
Figure S7. ^{1}H NMR spectrum of **S2** in CDCl$_3$.
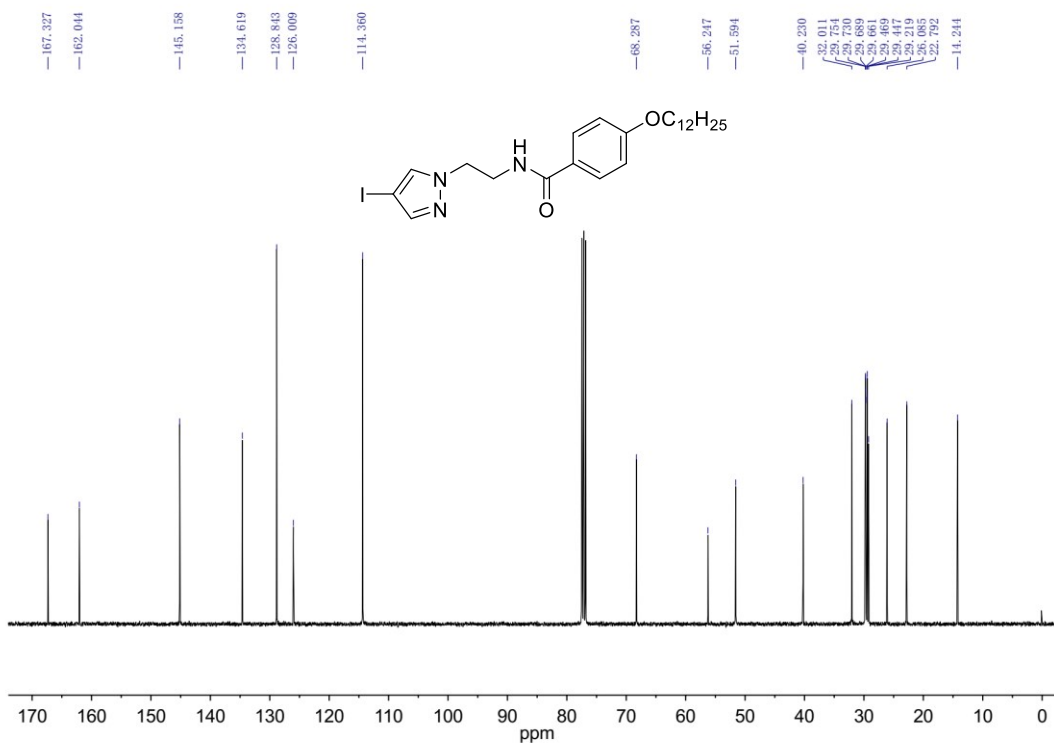
Figure S8. ^{13}C NMR spectrum of **S2** in CDCl$_3$.
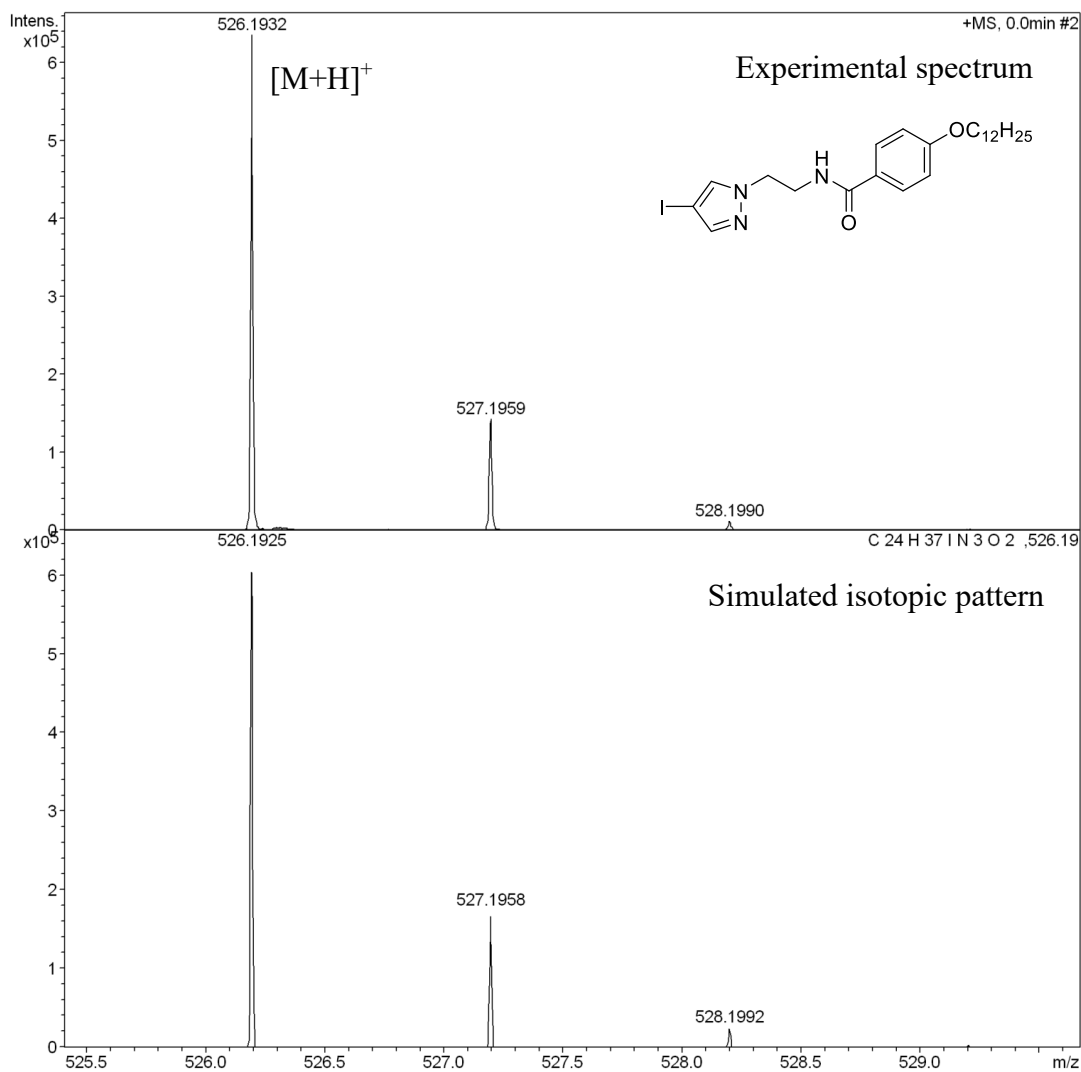
Figure S9. HRMS spectrum of **S2**.
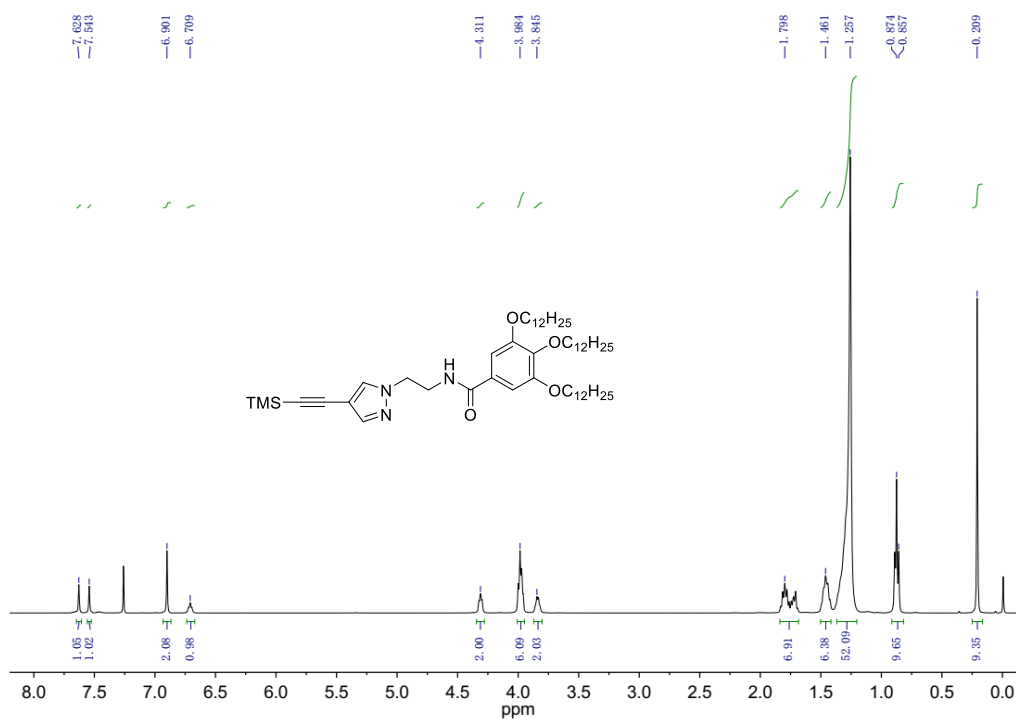
Figure S10. ^{1}H NMR spectrum of **S3** in CDCl$_3$.
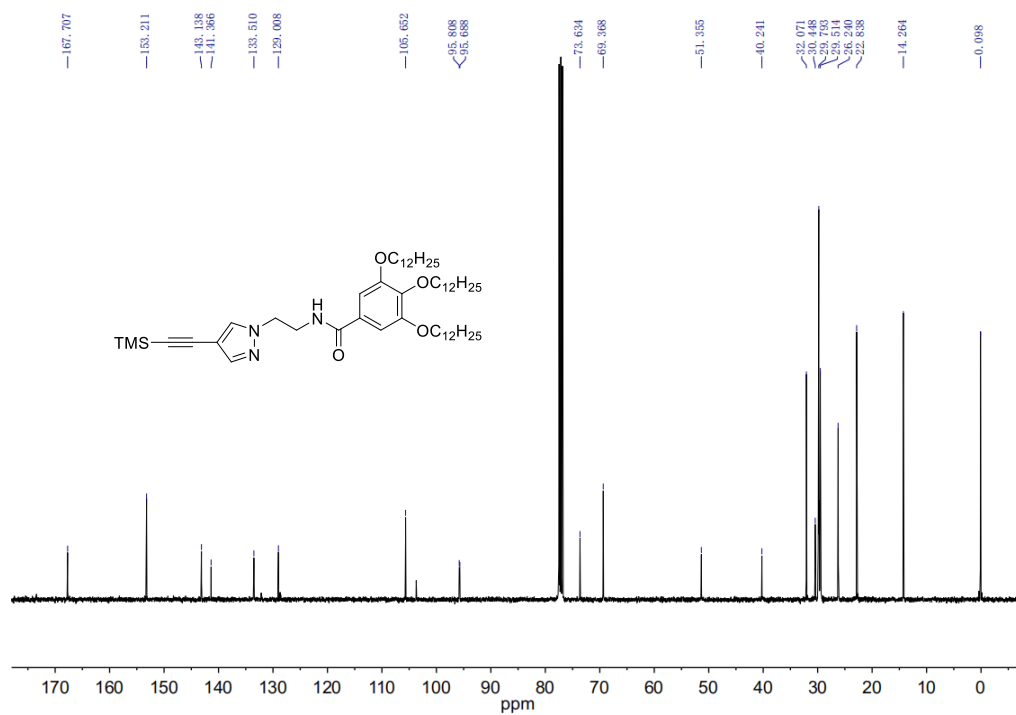
Figure S11. ^{13}C NMR spectrum of **S3** in CDCl$_3$.
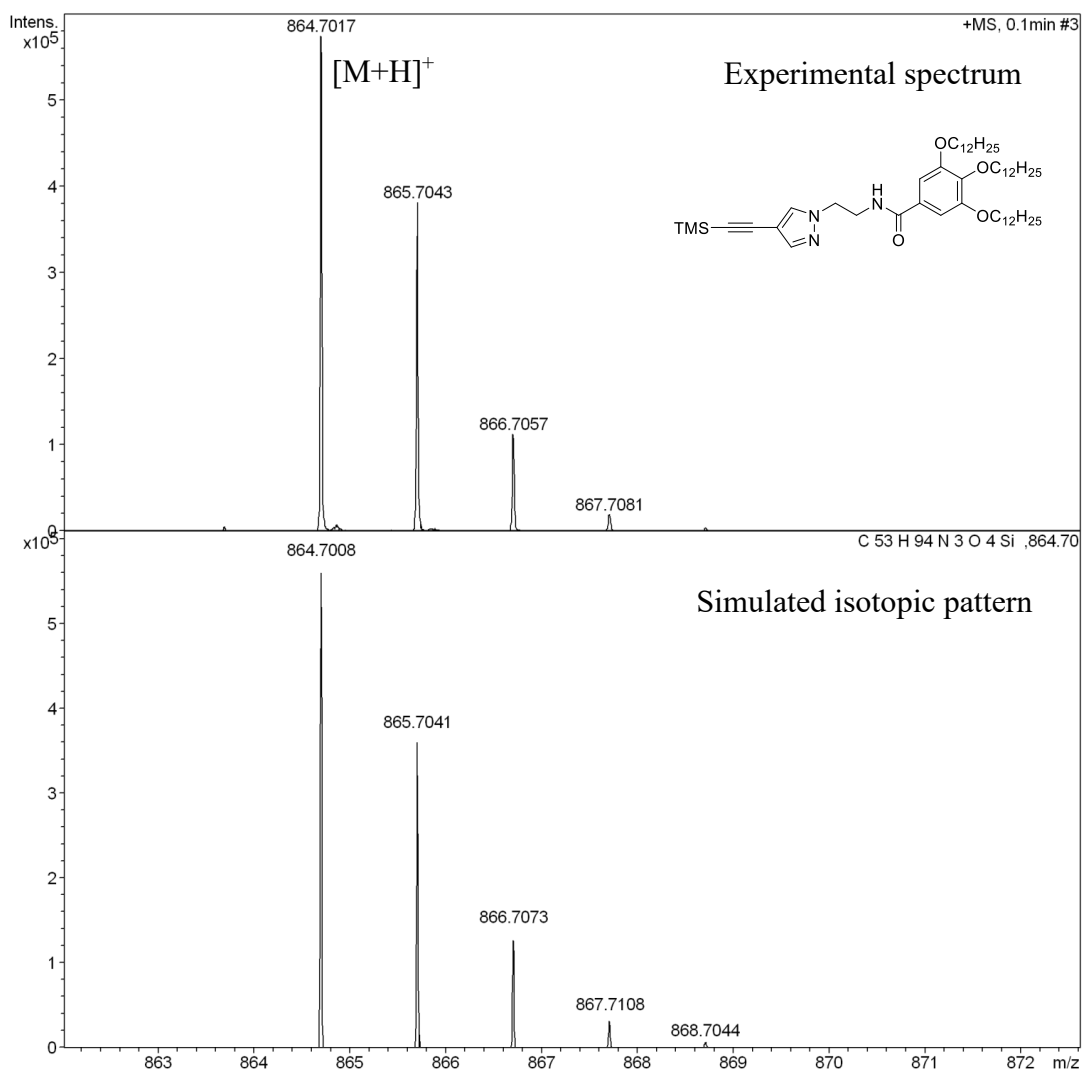
Figure S12. HRMS spectrum of **S3**.
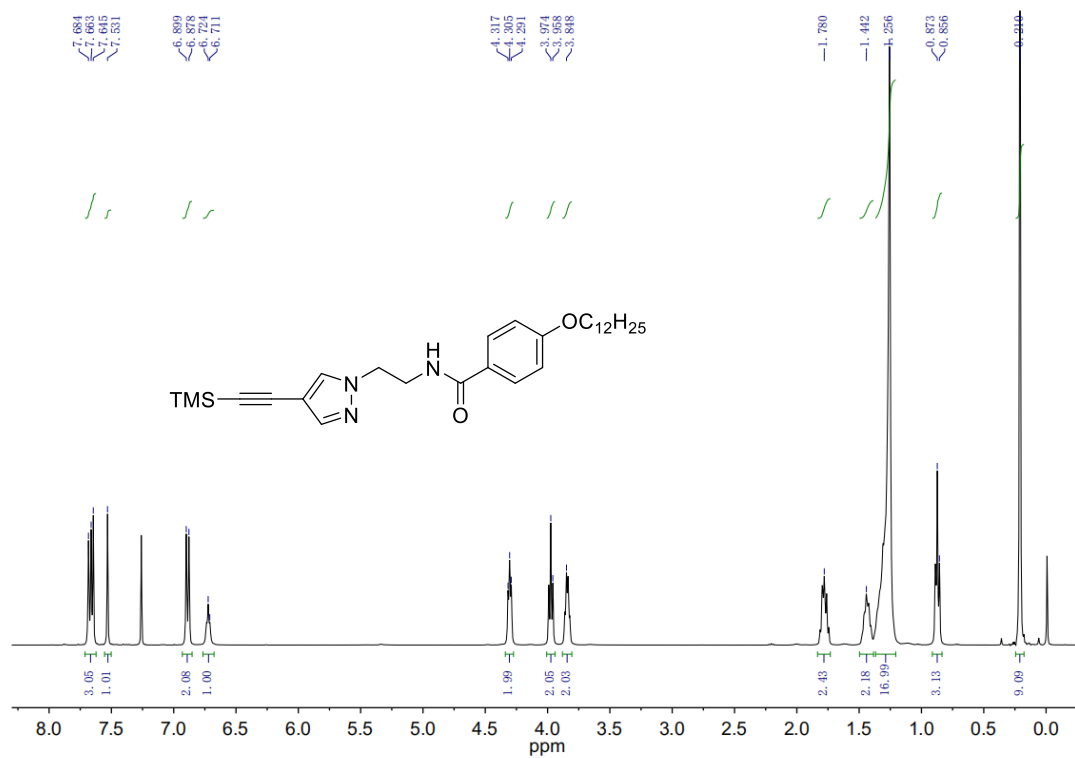
Figure S13. ^{1}H NMR spectrum of **S4** in CDCl$_3$.
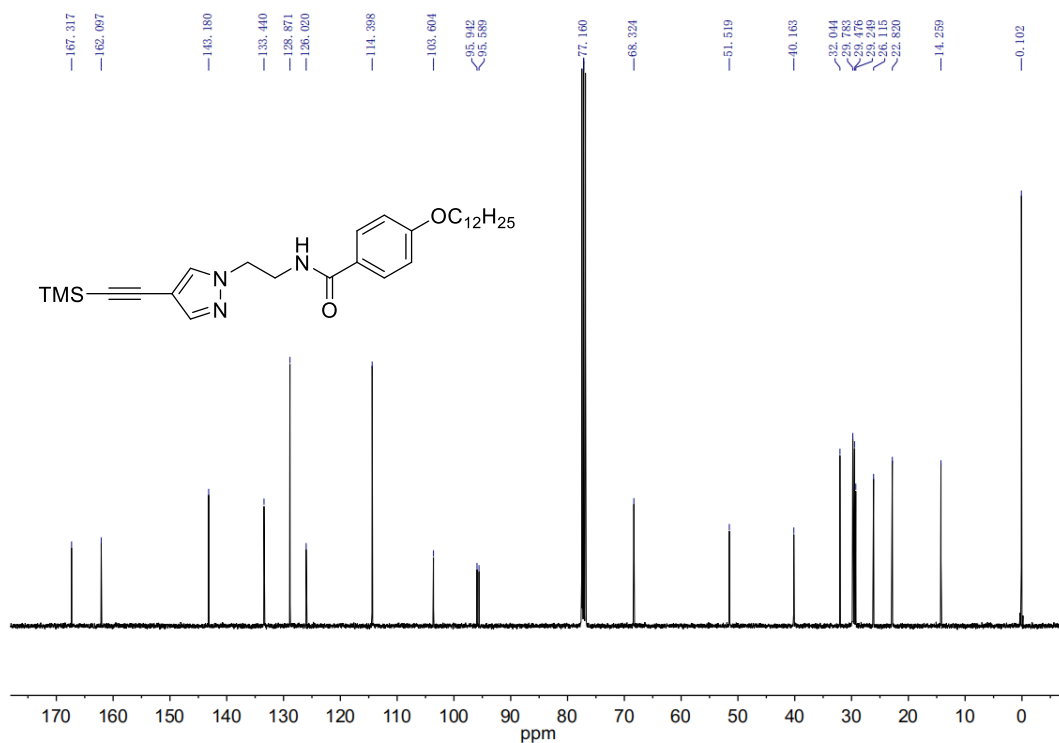
Figure S14. ^{13}C NMR spectrum of **S4** in CDCl$_3$.
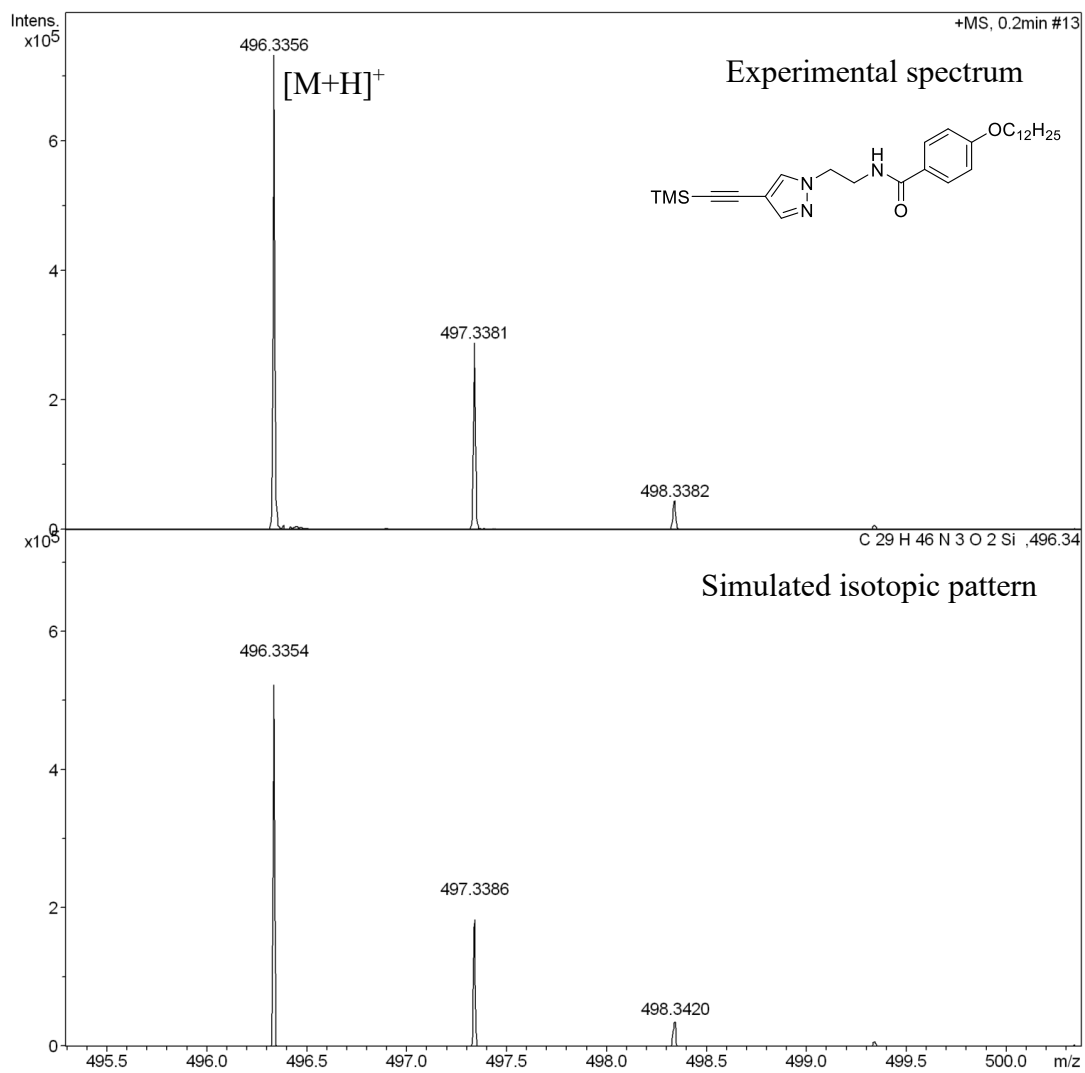
Figure S15. HRMS spectrum of **S4**.
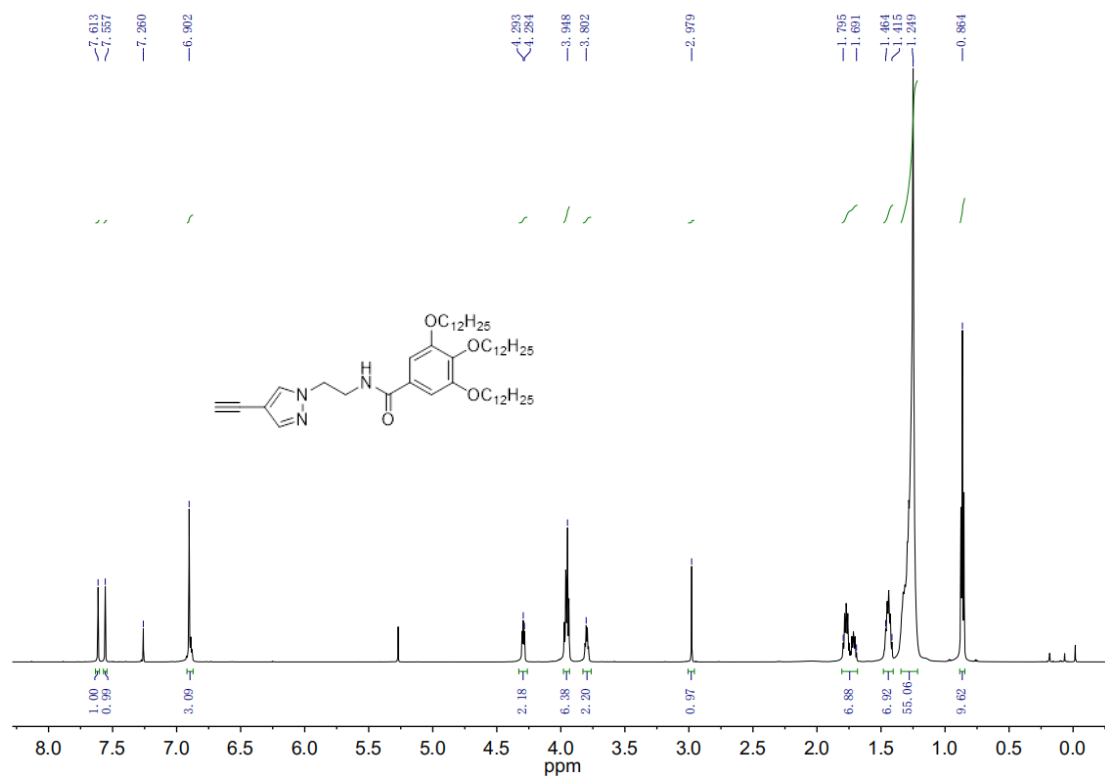
Figure S16. ^{1}H NMR spectrum of **M1** in CDCl$_3$.
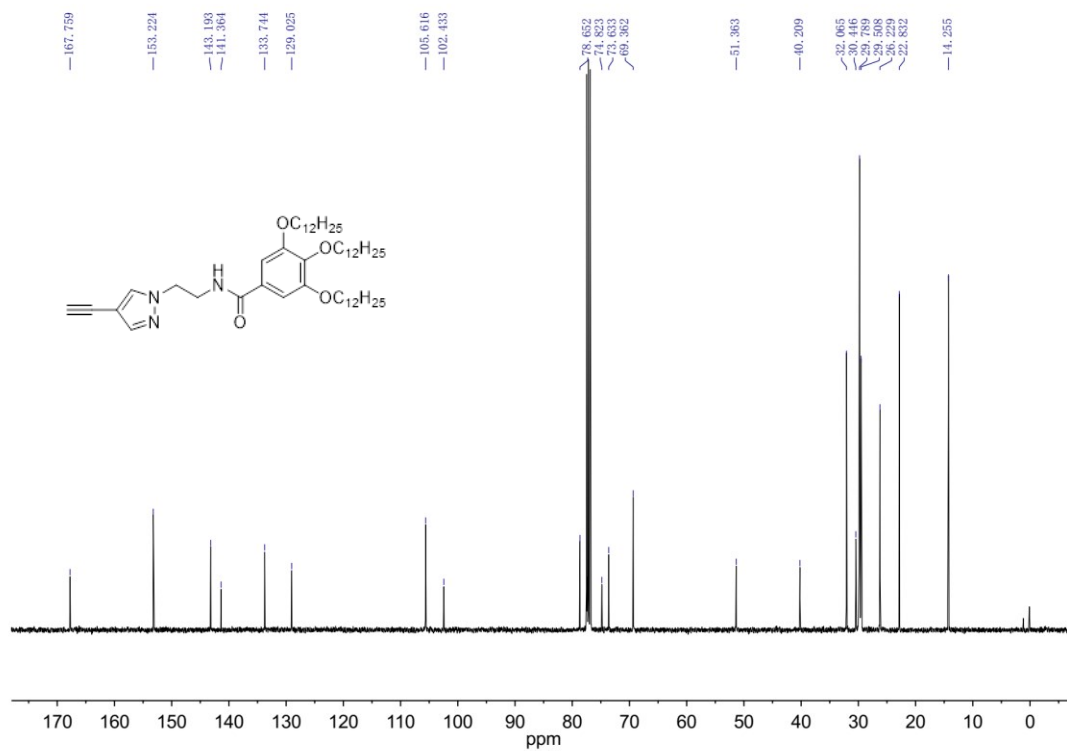
Figure S17. ^{13}C NMR spectrum of **M1** in CDCl$_3$.
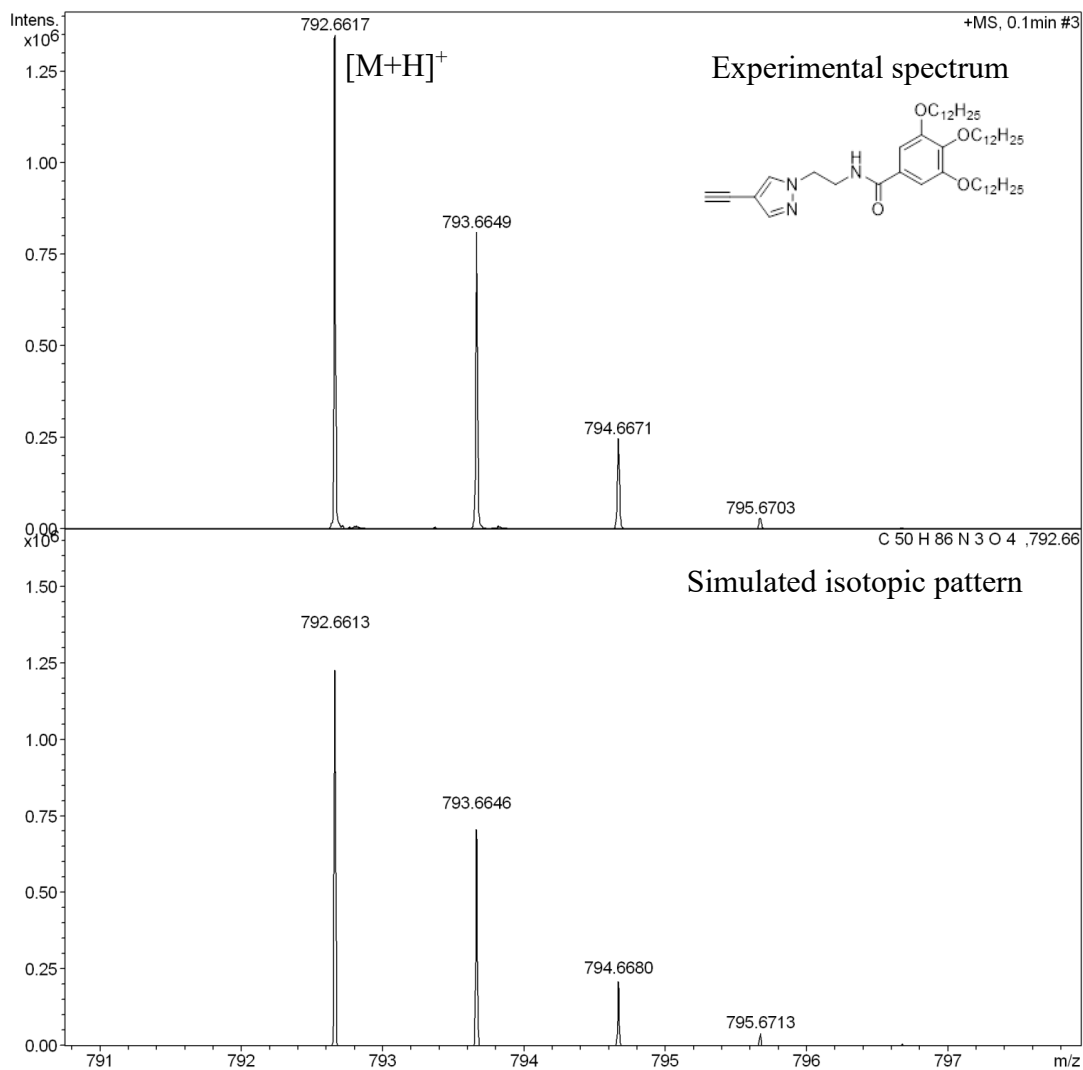
Figure S18. HRMS spectrum of **M1**.
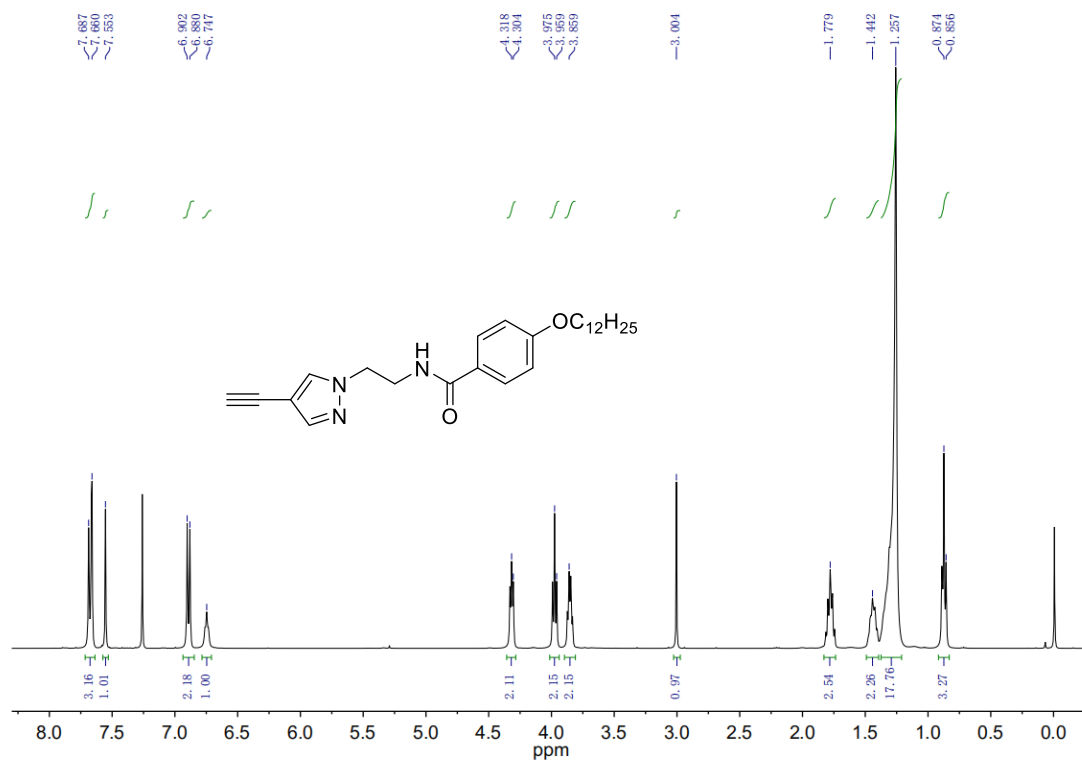
Figure S19. ^{1}H NMR spectrum of **M2** in CDCl$_3$.
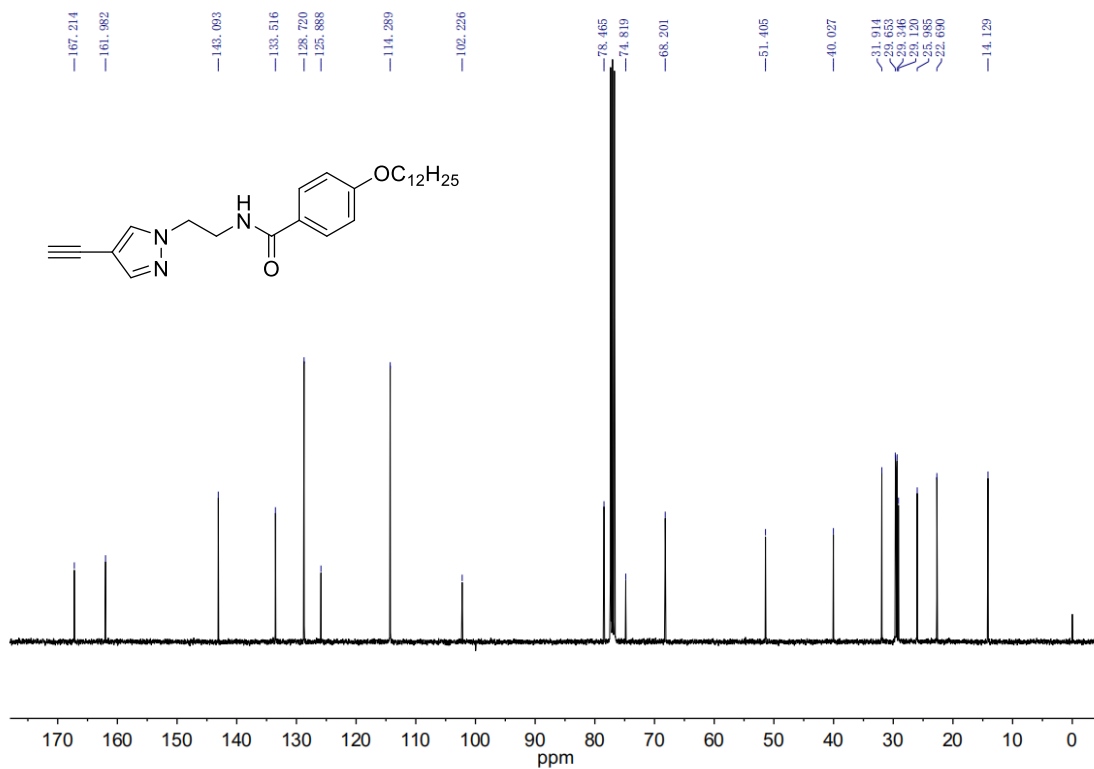
Figure S20. ^{13}C NMR spectrum of **M2** in CDCl$_3$.
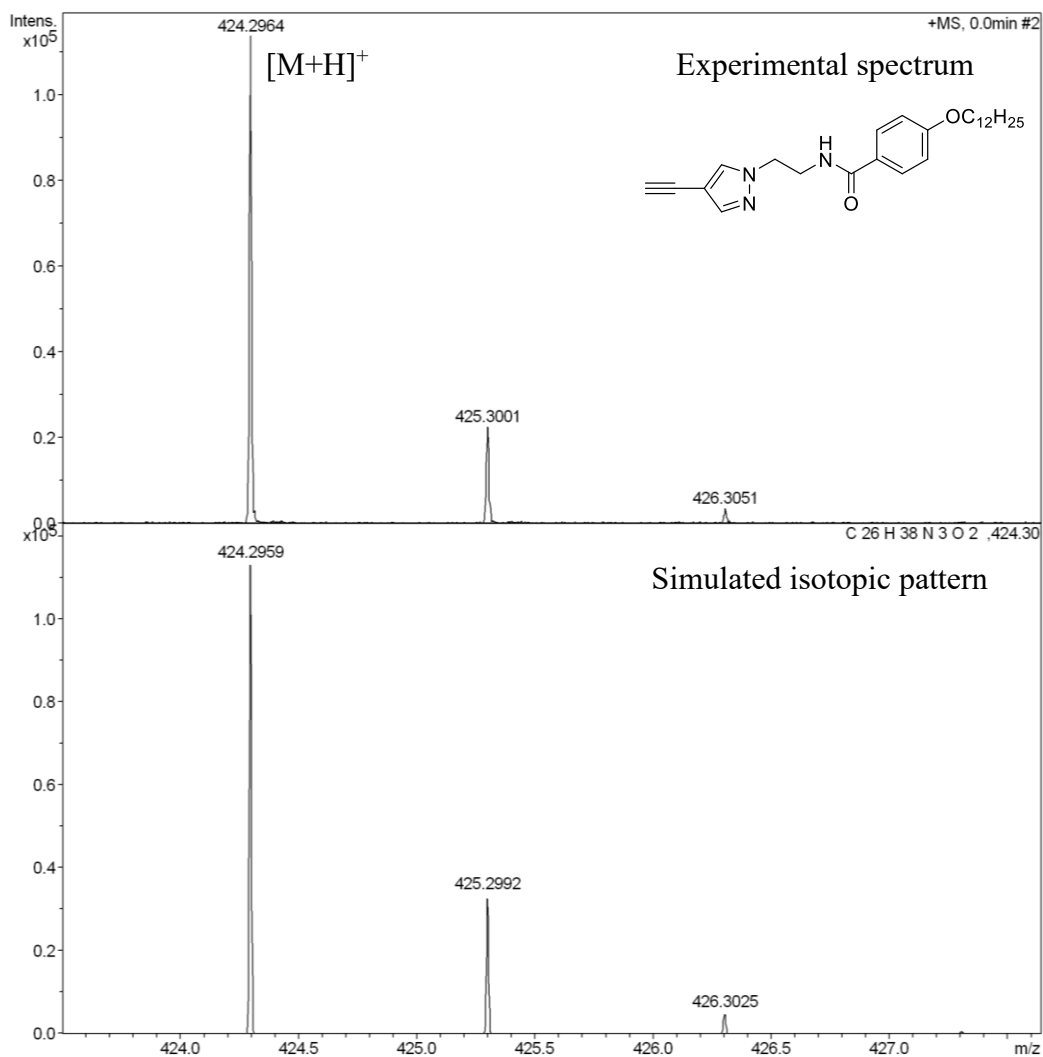
Figure S21. HRMS spectrum of **M2**.

Figure S22. ^{1}H NMR spectrum of **1** in CDCl$_3$.

Figure S23. ^{13}C NMR spectrum of **1** in CDCl$_3$.

Figure S24. HRMS spectrum of **1**.
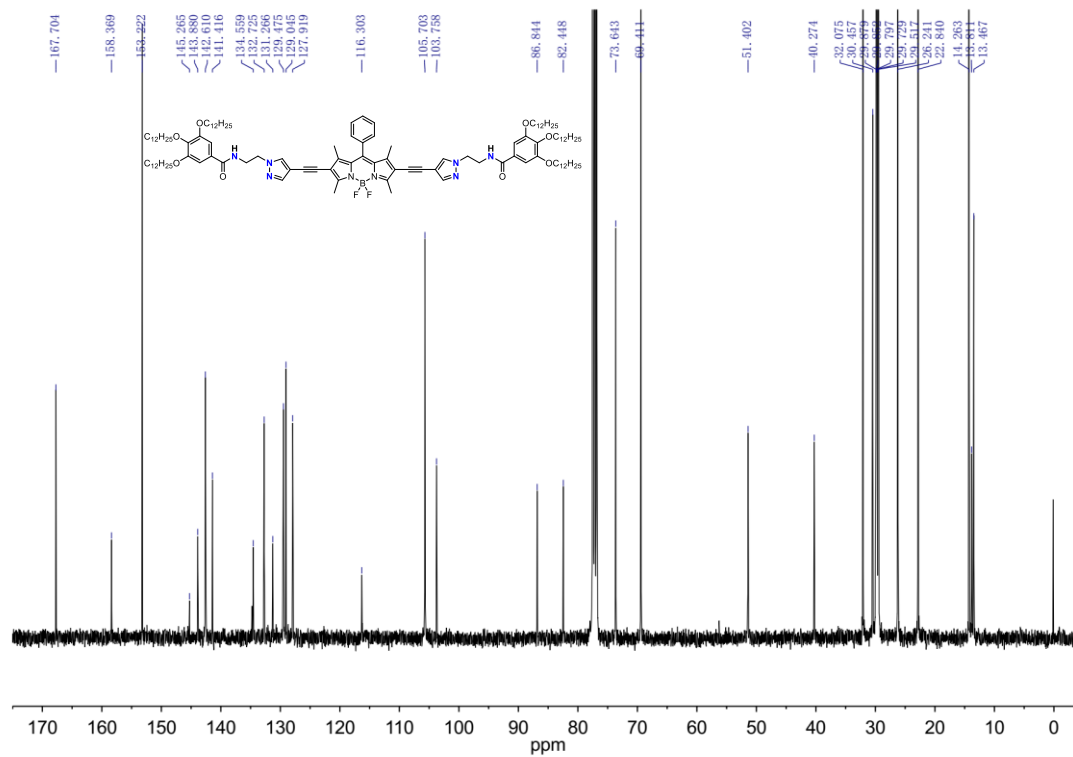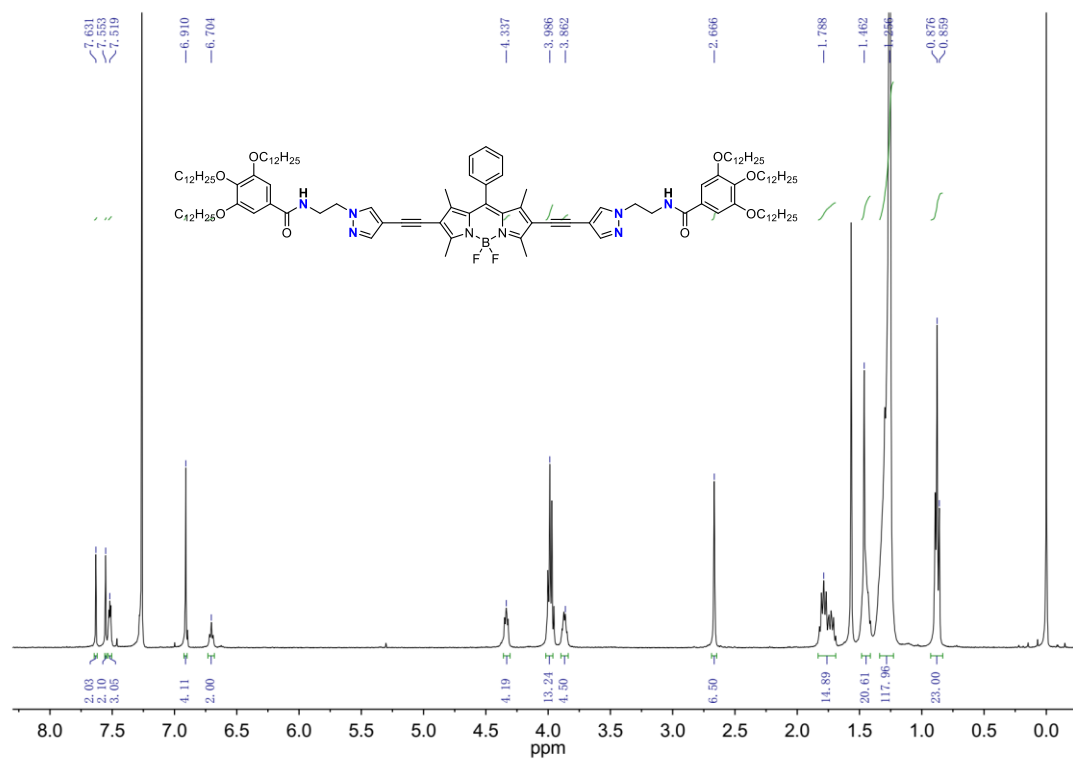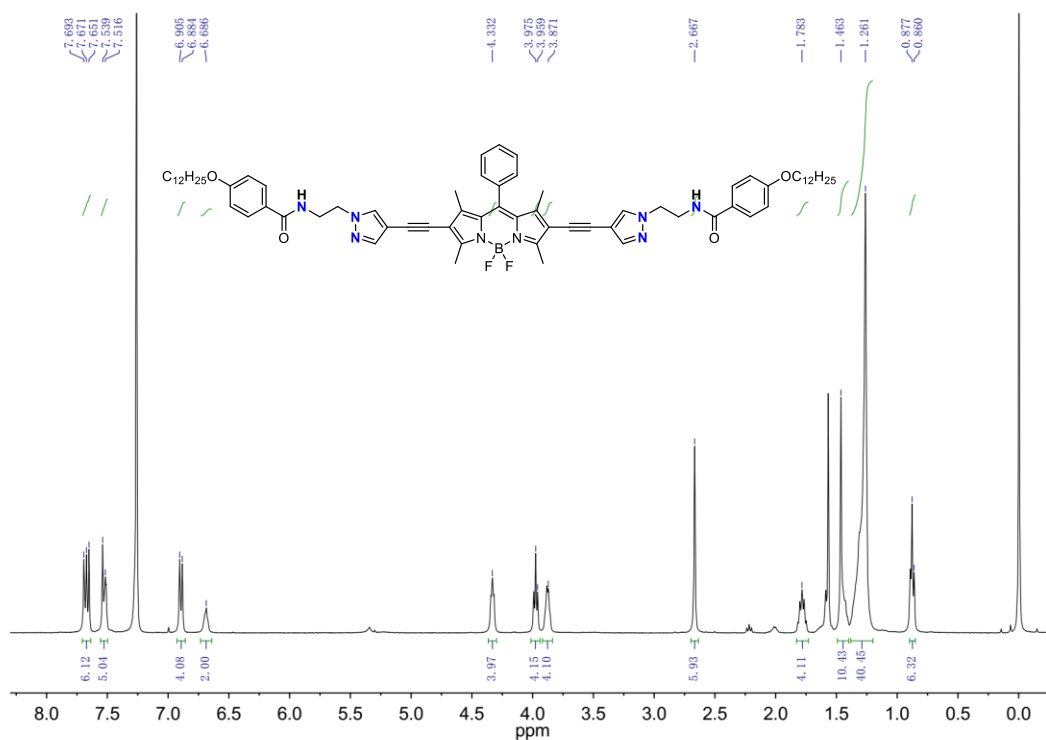
Figure S25. ^{1}H NMR spectrum of **2** in CDCl$_3$.
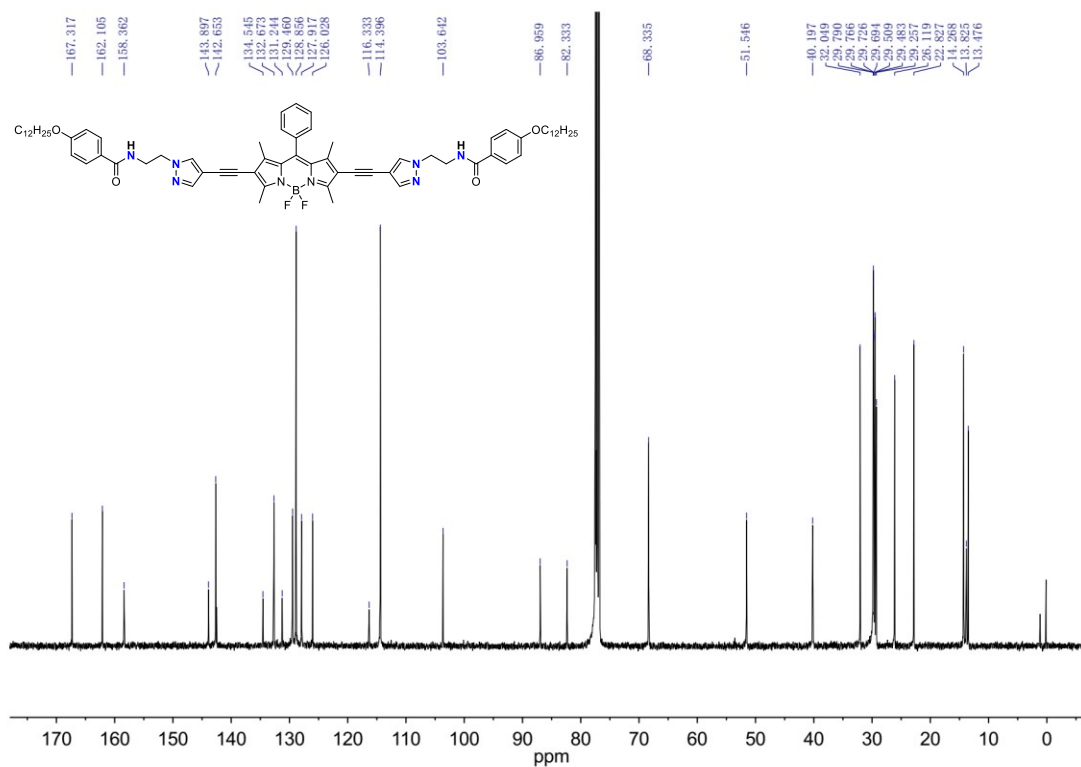
Figure S26. ^{13}C NMR spectrum of **2** in CDCl$_3$.
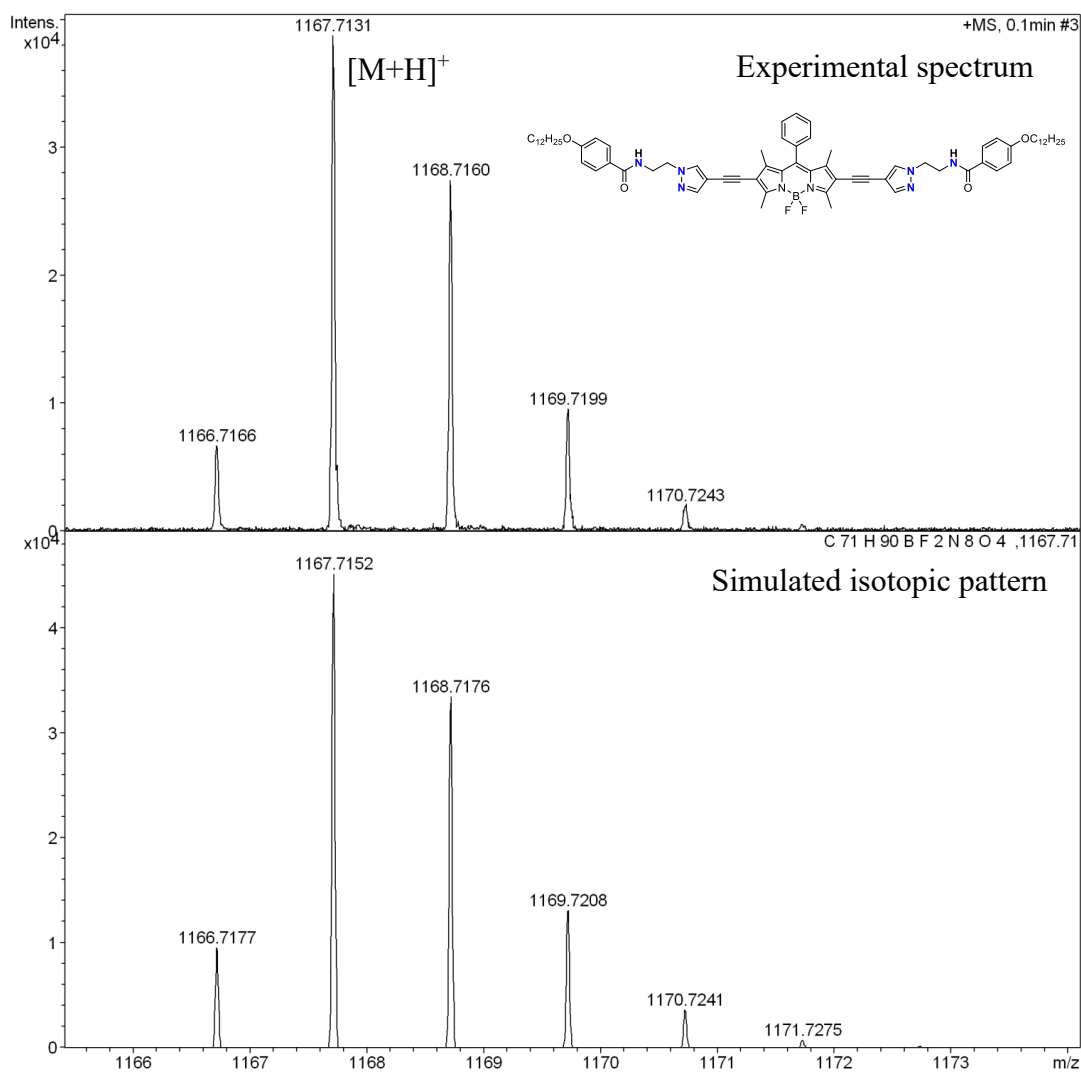
Figure S27. HRMS spectrum of **2**.
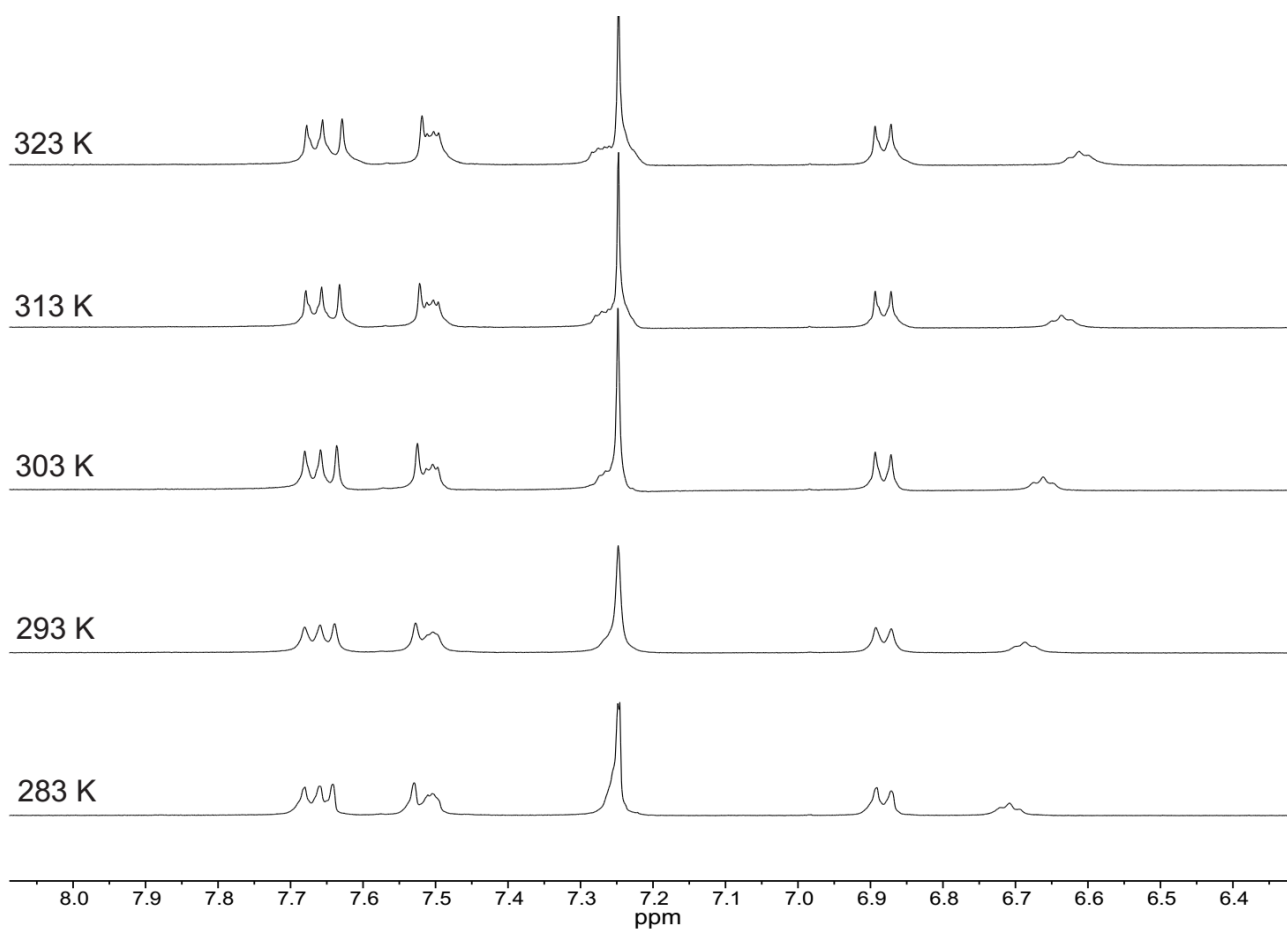
Figure S28. Temperature-dependent ^{1}H NMR spectra of **2** (4.0 mM) in CDCl$_3$.
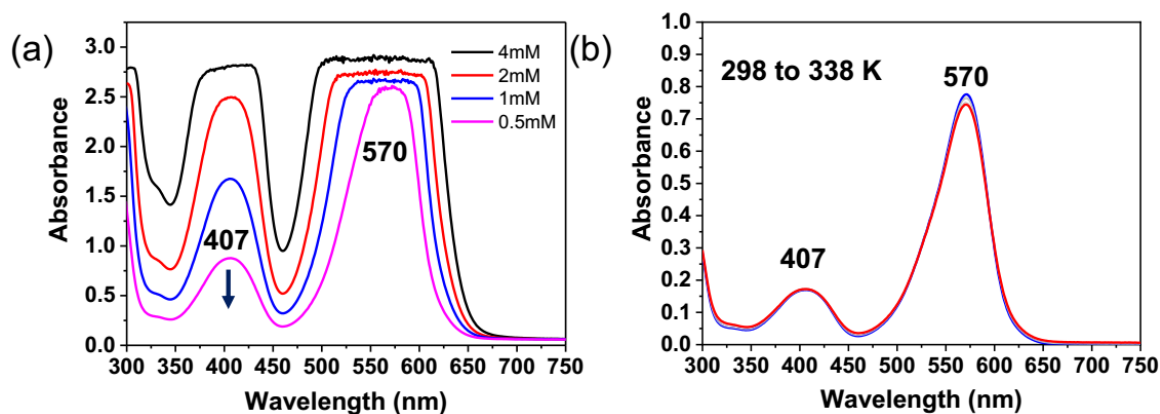
Figure S29. (a) Concentration-dependent UV-vis spectra of 2_{Mono} in CHCl₃ with 1 mm cuvette at 298 K; (b) Temperature-dependent UV-vis spectra of 2_{Mono} in CHCl₃ (c = 1.0 × 10^{-5} M).

Although 1mm cuvette was employed, the absorbance is still far out of the detection range at 4 mM, 2 mM and 1 mM. However, the absorption peak at ca. 407 is almost the same, and the major peaks give the very similar sharp in different concentration in CHCl₃, indicating that the monomeric species are dominant even at high concentration up to 4 mM (Fig. S29a).

In addition, we also tried the temperature dependent (298K to 338 K) UV-vis experiment (Fig. S29b), almost identical UV-vis profiles were observed for **2** in CHCl₃, indicating that the compound 2 is in monomeric state.
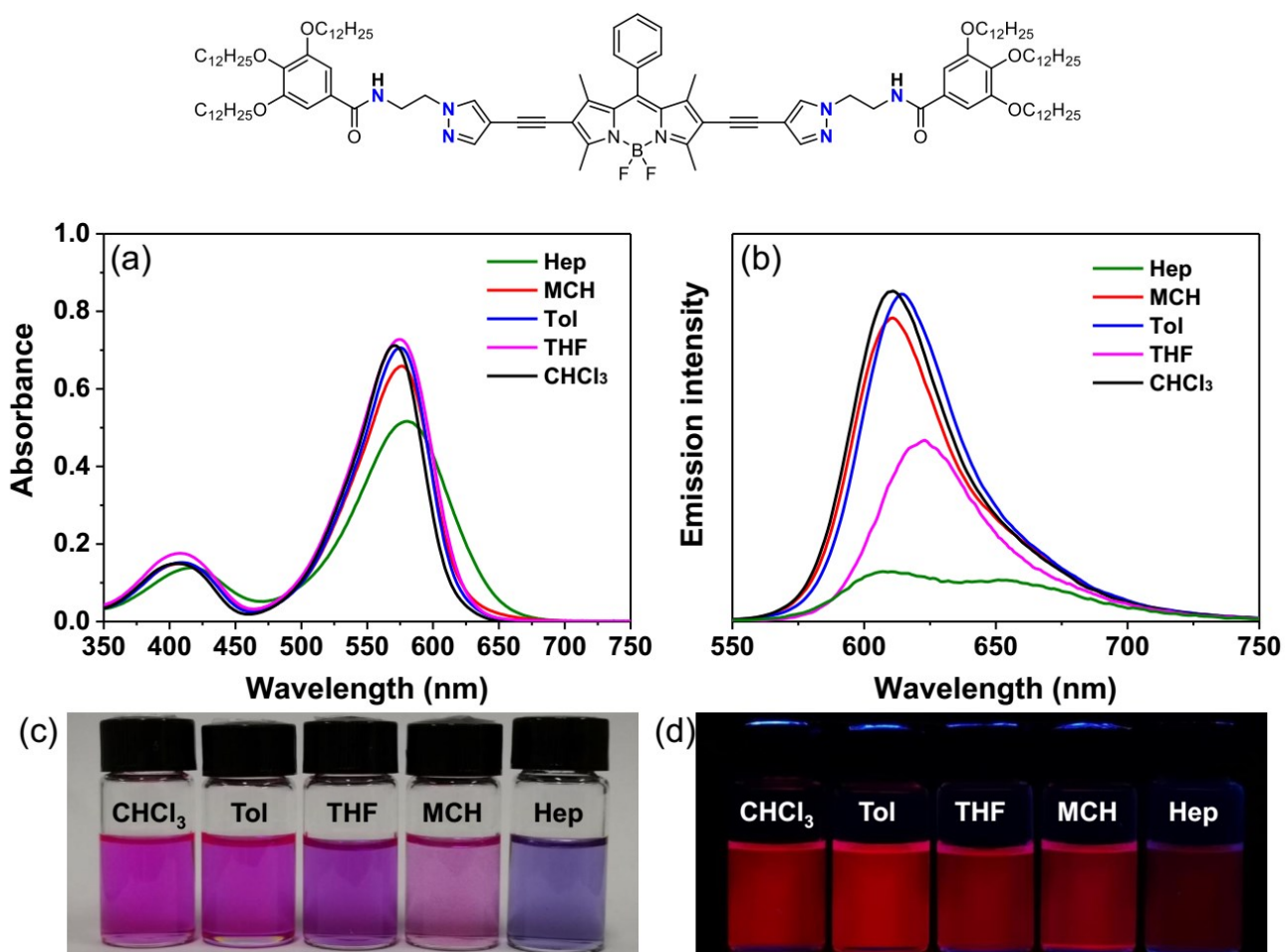
Figure S30. Photophysical properties of **1** (c = 1 × 10^{-5} M) in various solvents (CHCl$_3$, Toluene, THF, MCH and Heptane) at 298 K. (a) UV-vis absorption and (b) emission spectra, as well as (c, d) illustration of the solution colors (c) under ambient light and (d) UV-light.
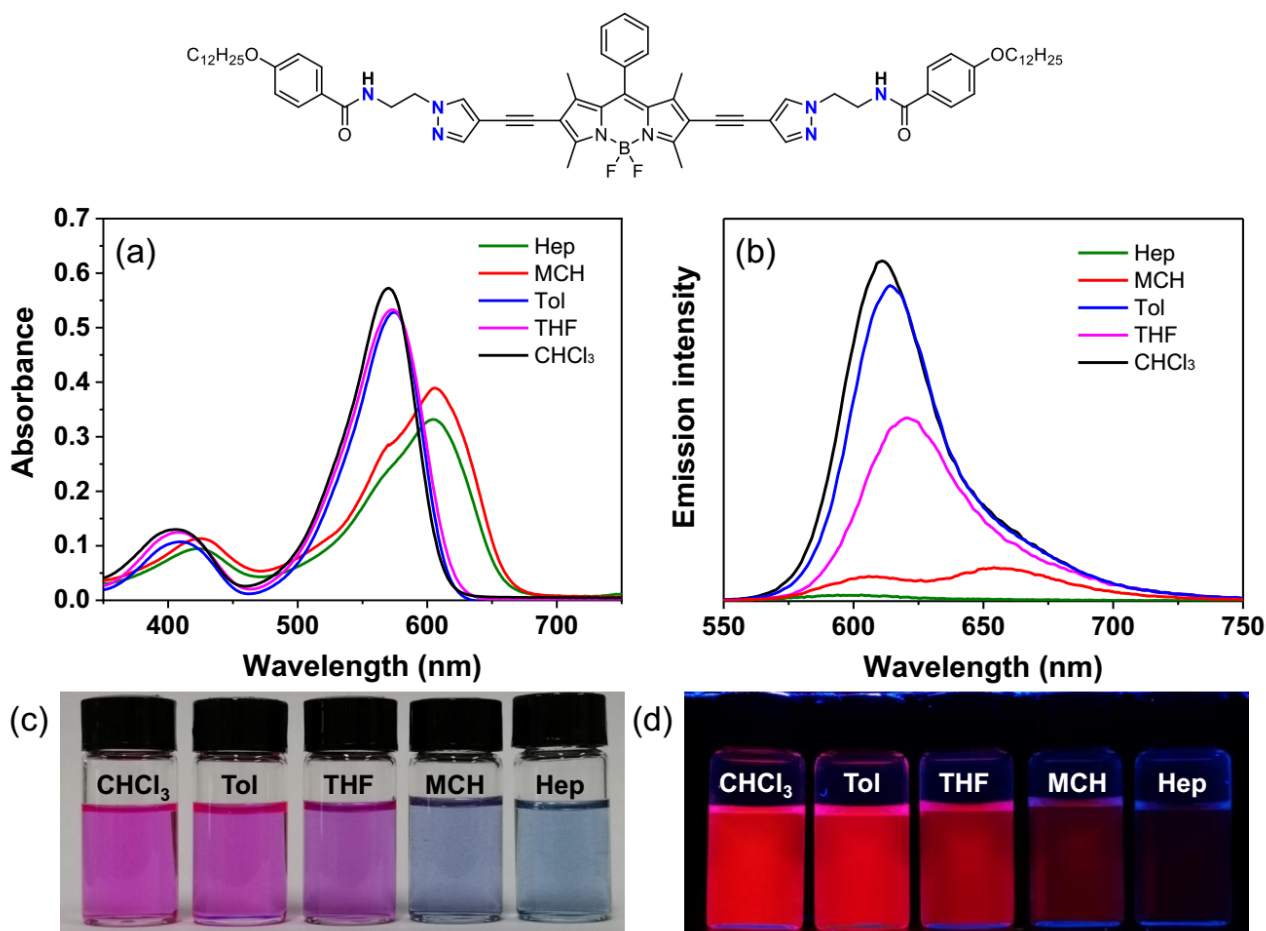
Figure S31. Photophysical properties of **2** (c = 1 × 10⁻⁵ M) in various solvents (CHCl₃, Toluene, THF, MCH and Heptane) at 298 K. (a) UV-vis absorption and (b) emission spectra, as well as (c, d) illustration of the solution colors (c) under ambient light and (d) UV-light.
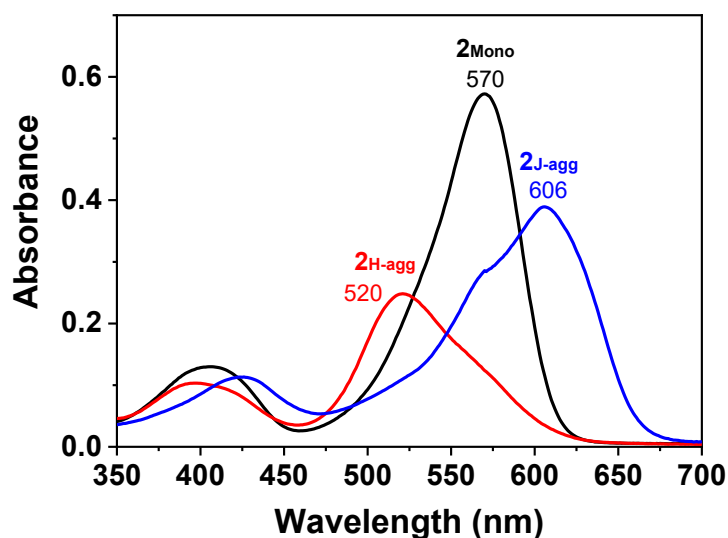
Figure S32. UV-vis absorption spectra of 2_{Mono} (black), 2_{J-agg} (blue) and 2_{H-agg} (red) in MCH (1×10^{-5} M). 2_{Mono} was prepared by heating the MCH solution to 353 K; 2_{J-agg} was prepared by cooling from 353 K to 288 K; and 2_{H-agg} was prepared by the stirring of the MCH solution of 2_{J-agg} at 288 K overnight.
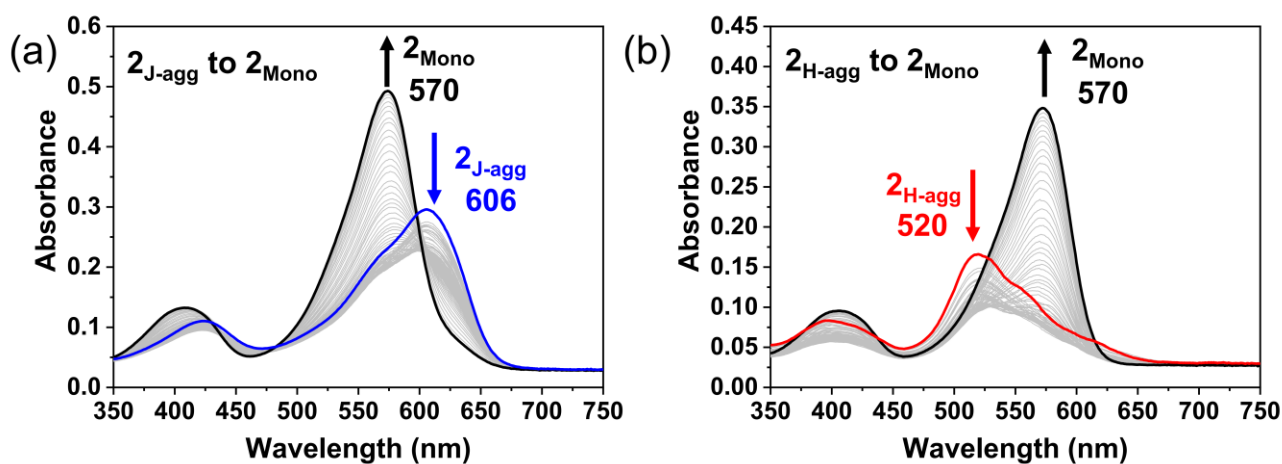
Figure S33. (a) Temperature-dependent UV-vis absorption spectra of 2_{J-agg} in MCH (c = 1×10^{-5} M) upon heating from 288 K to 353 K with a rate of 1 K min^{-1} showing the showing the transformation from 2_{J-agg} (blue line) to 2_{Mono} (black line). (b) Temperature-dependent UV/Vis absorption spectra of 2_{H-agg} in MCH (c = 1×10^{-5} M) upon heating from 288 K to 353 K with a rate of 1 K min^{-1} showing the showing the transformation from 2_{H-agg} (red line) to 2_{Mono} (black line).
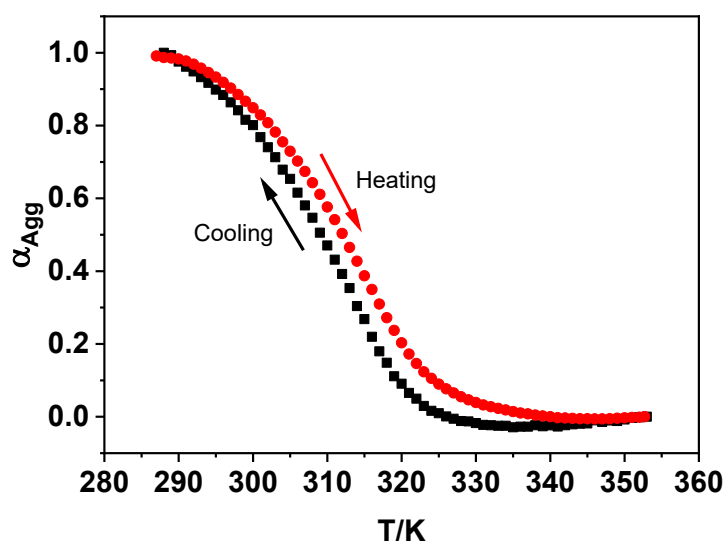
Figure S34. (a) Temperature-dependent degree of $1_{J\text{-Agg}}$ (α_{agg}) calculated from the absorption at $\lambda =$ 560 nm observed in the cooling (black) and heating (red) processes at a rate of 1 K min^{-1}. Condition: c = 1.0×10^{-5} M in heptane.
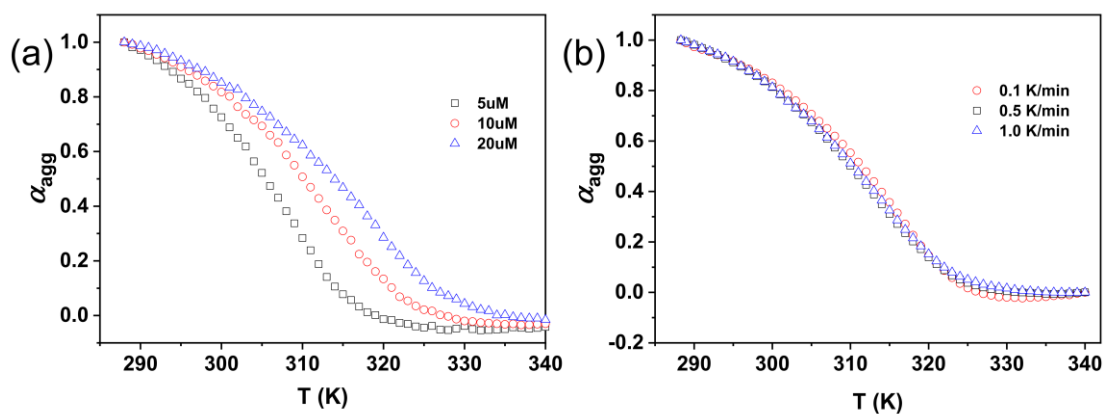
Figure S35. Plot of a_{agg} of $1_{J\text{-Agg}}$ monitored at 560 nm versus temperatures upon cooling at various concentrations of **1** in heptane. (b) Plot of a_{agg} of $1_{J\text{-Agg}}$ monitored at 560 nm versus temperatures upon cooling the heptane solution of **1** (c = 1.0×10^{-5} M) with different cooling rate.

Increasing the concentration leads to higher T_m (temperature at which α_{agg} is 0.5) values; while decreasing the cooling rate from 1 to 0.1 K/min^{-1} exerts little effect of T_m.
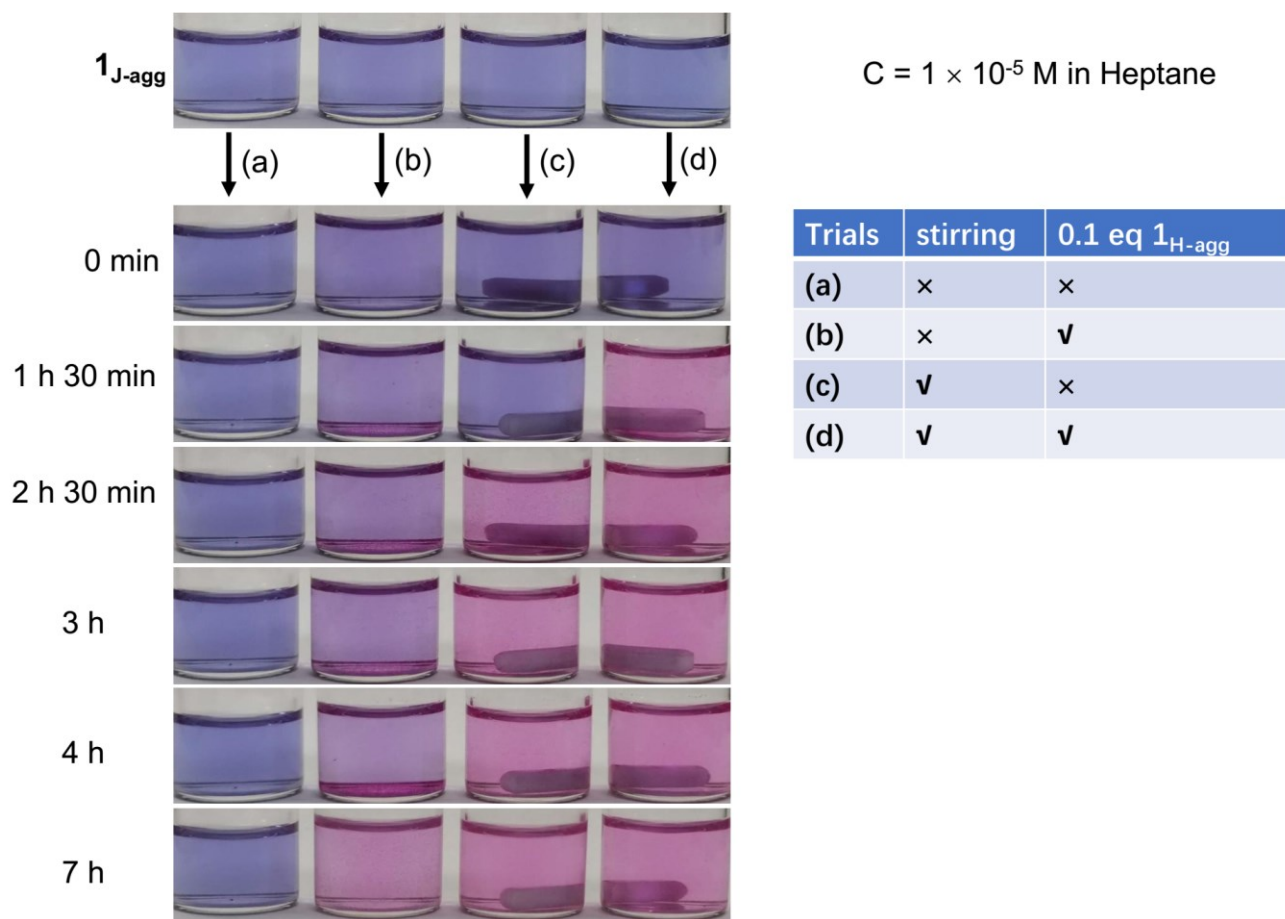
Figure S36. Photographs of the solutions showing the transformation from **1**_{J-agg} to **1**_{H-agg} in heptane under different agitation.
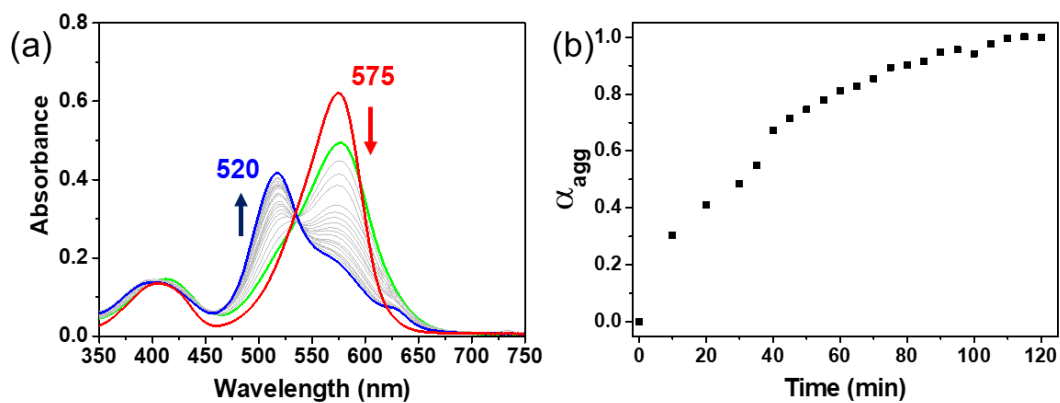
Figure S37. (a) Temperature-dependent UV-vis absorption spectra of **1** in heptane (c = 1.0 × 10^{-5} M) showing the transformation from **1$_{Mono}$** to **1$_{H-agg}$** directly. Firstly, **1** heptane solution (c = 1.0 × 10^{-5} M) was cooled from 353 K (red line) to 308 K (green line) (10 K min^{-1}). Then the seeds of **1$_{H-agg}$** was added, followed by cooling to 298 K (10 K min^{-1}). Finally, **1$_{H-agg}$** was observed in ca. 2h (blue line). (b) Degree of **1$_{H-agg}$** (α_{agg}) monitored at 560 nm versus time observed in **1** in heptane (c = 1.0 × 10^{-5} M) at 298 K.
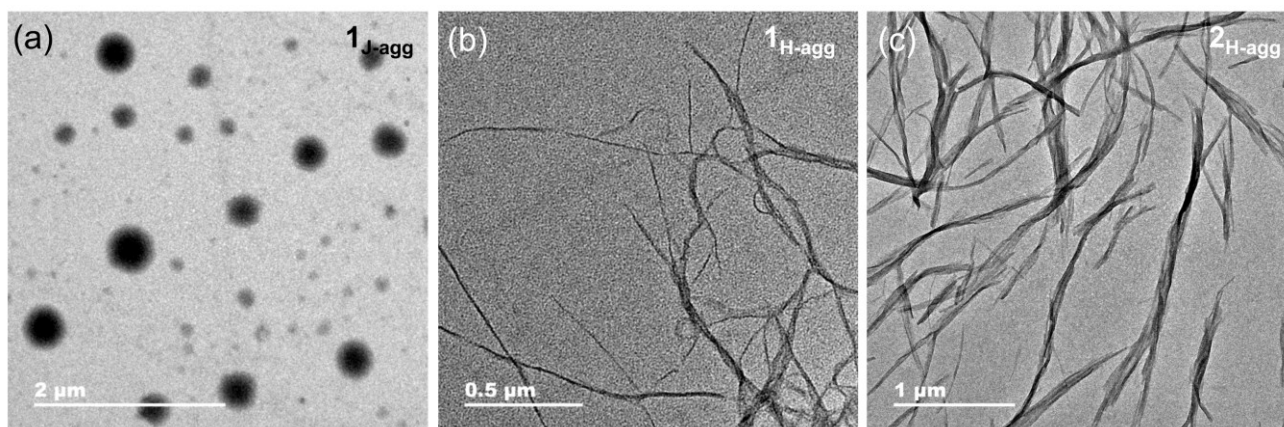
Figure S38. TEM images of (a) **1$_{J-agg}$**, (b) **1$_{H-agg}$** and **2$_{H-agg}$**.
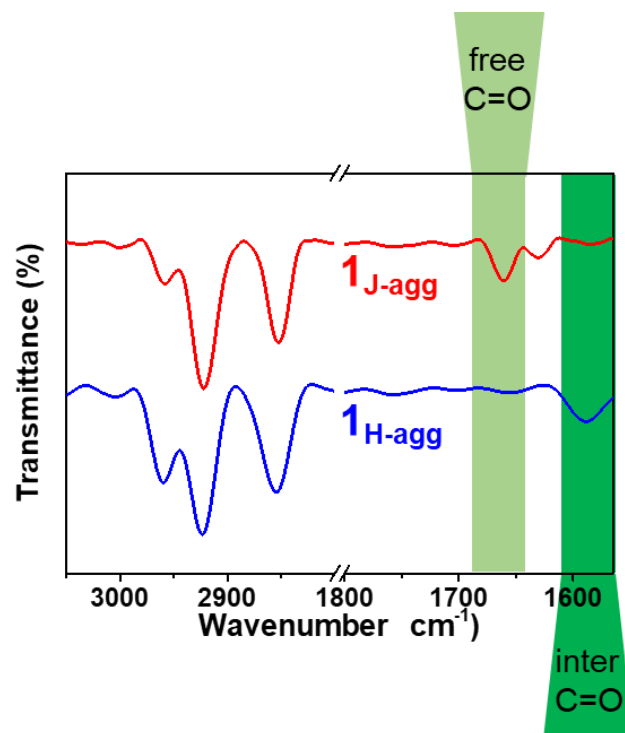
Figure S39. FT-IR spectra of **1J-agg** and **1H-agg**.
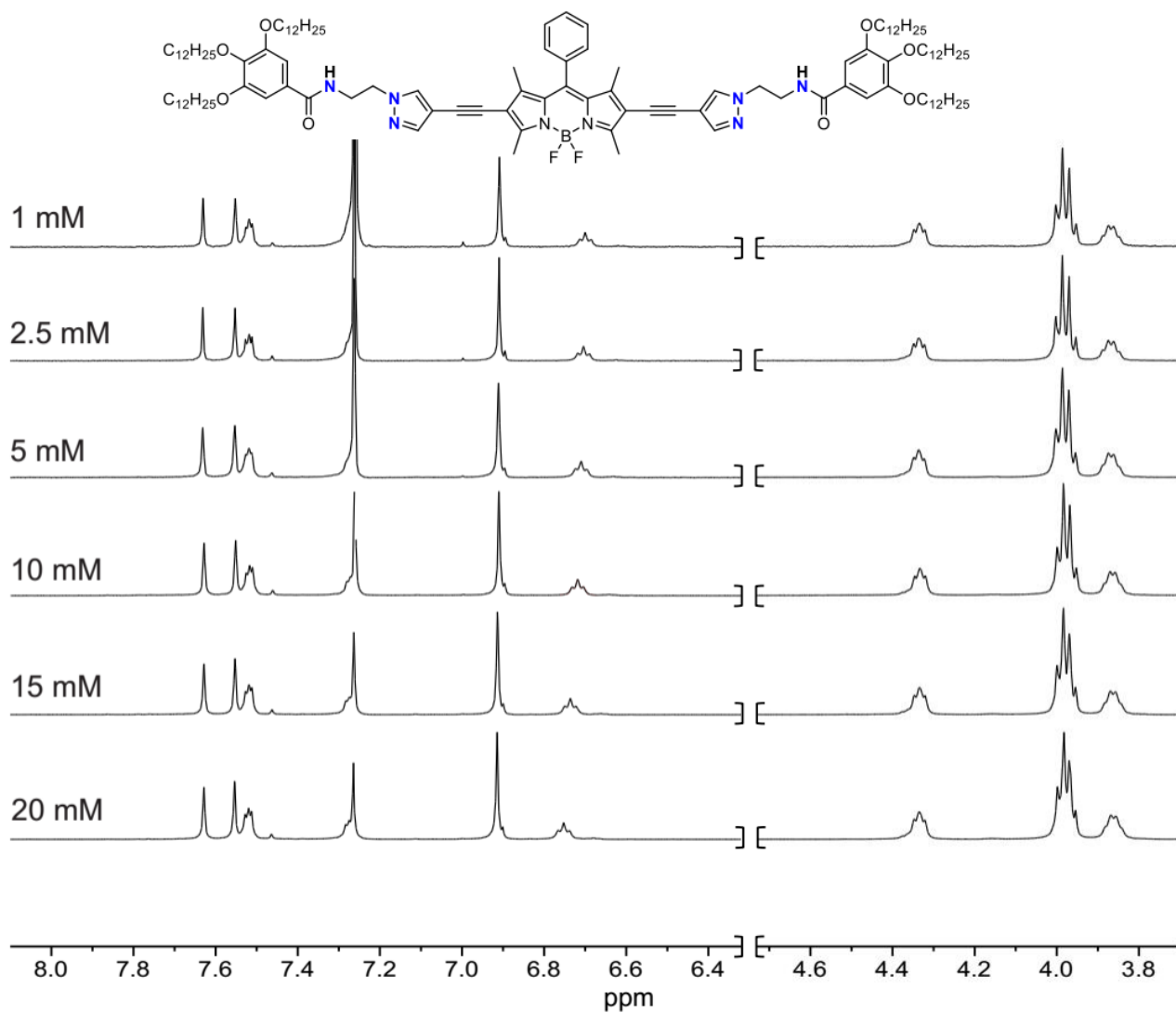
Figure S40. Concentration-dependent ^{1}H NMR spectra of **1** in CDCl$_3$ at 298 K.
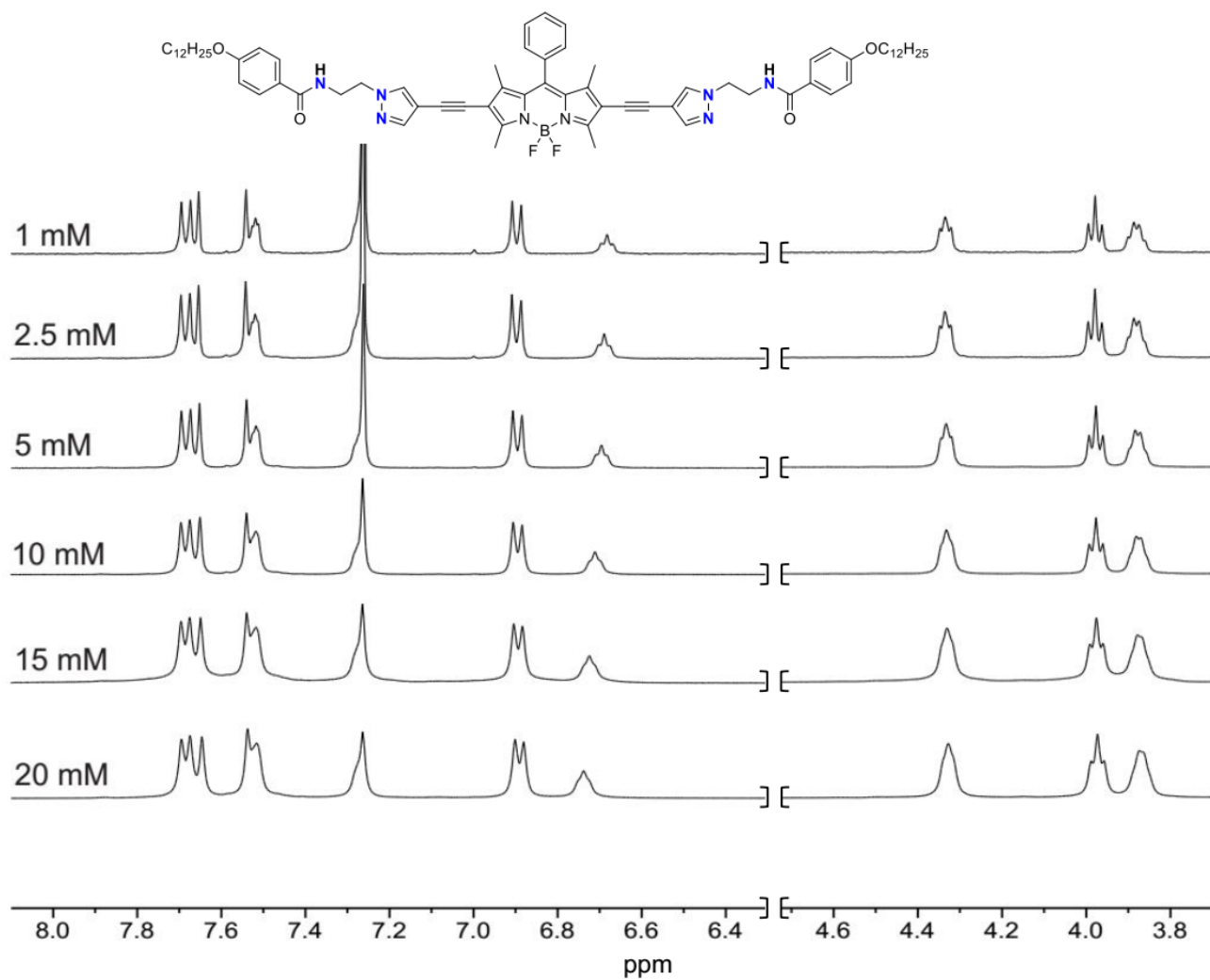
Figure S41. Concentration-dependent ^{1}H NMR spectra of **2** in CDCl$_3$ at 298 K.
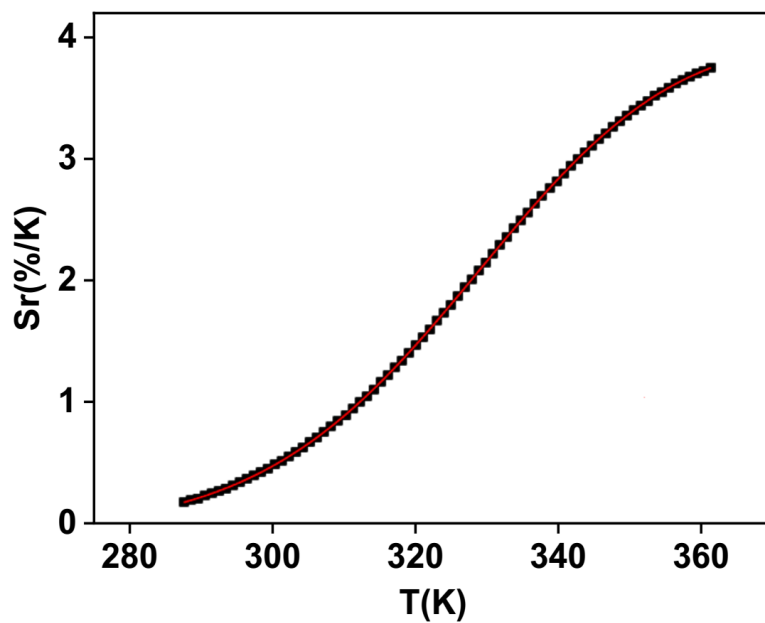
Figure S42. S_r values at varying temperature (288-363 K) for **1** (black symbols) and the red line is a fit curve.
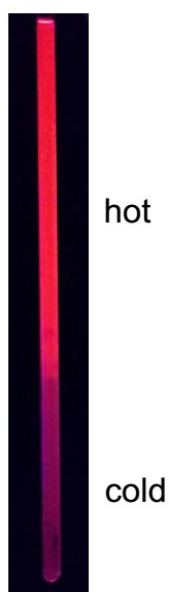
Figure S43. Photographs of the solutions showing the various emission of **1** in Heptane.

Table S1. Photophysical data for **1**–**2**.

Compounds	Solvents	λ_{abs}/nm ($\varepsilon \times 10^{-4}$ / dm^3 mol^{-1} cm^{-1})	λ_{em}/nm (Φ_F)
1	Heptane	417 (1.39), 581 (5.16)	607, 654 (0.03)
	MCH	409 (1.99), 576 (6.59)	611 (0.12)
	Toluene	410 (1.52), 575 (7.06)	614 (0.25)
	Tetrahydrofuran	408 (1.76), 574 (7.28)	623 (0.07)
	CHCl$_3$	406 (1.60), 575 (7.12)	611 (0.13)
2	Heptane	422 (0.95), 605 (3.31)	603 (0.01)
	MCH	426 (1.13), 606 (3.89)	607, 655 (0.05)
	Toluene	409 (1.07), 574 (5.28)	614 (0.26)
	Tetrahydrofuran	409 (1.25), 573 (5.33)	621 (0.09)
	CHCl$_3$	406 (1.30), 570 (5.72)	610 (0.33)

Reference:

S1. (a) W. Wu, J. Zhao, H. Guo, J. Sun, S. Ji and Z. Wang, *Chem. Eur. J.*, 2012, **18**, 1961-1968; (b) M. Gorbe, A. M. Costero, F. Sancenón, R. Martínez-Máñez, R. Ballesteros-Cillero, L. E. Ochando, K. Chulvi, R. Gotor and S. Gil, *Dyes Pigm.*, 2019, **160**, 198-207.

S2. (a) A. Rödle, B. Ritschel, C. Mück-Lichtenfeld, V. Stepanenko and G. Fernández, *Chem. Eur. J.*, 2016, **22**, 15772-15777; (b) J. Fan, X. Chang, M. He, C. Shang, G. Wang, S. Yin, H. Peng and Y. Fang, *ACS Appl. Mater. Interfaces*, 2016, **8**, 18584-18592; (c) K. R. Reddy, E. Varathan, N. P. Lobo, S. Easwaramoorthi and T. Narasimhaswamy, *J. Phys. Chem. C*, 2016, **120**, 22257-22269.

S3. M. M. J. Smulders, M. M. L. Nieuwenhuizen, T. F. A. de Greef, P. van der Schoot, A. P. H. J. Schenning and E. W. Meijer, *Chem. Eur. J.*, 2010, **16**, 362-367.

S4. P. Jonkheijm, P. van der Schoot, A. P. H. J. Schenning and E. W. Meijer, *Science*, 2006, **313**, 80-83.

S5. A. M. Kaczmarek, R. Van Deun and M. K. Kaczmarek, *Sensor. Actuator. B Chem.*, 2018, **273**, 696-702.

S6. A. M. Kaczmarek, Y.-Y. Liu, M. K. Kaczmarek, H. Liu, F. Artizzu, L. D. Carlos and P. Van Der Voort, *Angew. Chem. Int. Ed.*, 2020, **59**, 1932-1940.

S7. D. Errulat, R. Marin, D. A. Gálico, K. L. M. Harriman, A. Pialat, B. Gabidullin, F. Iikawa, O. D. D. Couto, J. O. Moilanen, E. Hemmer, F. A. Sigoli and M. Murugesu, *ACS Cent. Sci.*, 2019, **5**, 1187-1198.